# ACTIVATED CARBON FROM PGX POLYMERS

# TOWARDS THE CREATION OF POROUS CARBON MATERIALS FROM POLYSACCHARIDE PRECURSORS: FEASIBILITY OF PGX PROCESSED POLYMERS FOR THE PRODUCTION OF ACTIVATED CARBON

By INDRANIL SARKAR, B.Eng.

A Thesis Submitted to the School of Graduate Studies in Partial Fulfillment of the Requirements for the Degree Master of Applied Science

MASTER OF APPLIED SCIENCE (2018) McMaster University

(Chemical Engineering) Hamilton, Ontario

| | |
|---|---|
| TITLE | Towards the creation of porous carbon materials from polysaccharide precursors: Feasibility of PGX processed polymers for the production of activated carbon |
| AUTHOR | Indranil Sarkar<br>B.Eng. (Manipal Institute of Technology, India) |
| SUPERVISOR | Dr. David Latulippe |
| NUMBER OF PAGES | xvii,103 |

# Lay Abstract

Activated carbon refers to a broad range of porous solids that find application in various industries, particularly for purification processes. Primarily produced from coal, there is a growing demand for finding sustainable alternatives. In this work, an attempt was made to produce activated carbon from polysaccharides (starch and pectin), which are naturally abundant bio-polymers. This thesis investigates 1) Comparative study between PGX processed and unprocessed polymers (starch and pectin) for the production of activated carbon. 2) Optimization study for manufacturing of high surface area activated carbon from pectin. Gas sorption measurements and SEM analysis revealed that while starch was unsuitable for production of activated carbon, high surface area carbon can be produced using chemically activated pectin. The carbon produced had a high degree of microporosity and preliminary adsorption tests for removal of heavy metal ions from water revealed promising adsorption capacities.

# Abstract

This thesis investigates the feasibility of producing activated carbon from polysaccharides. Activated carbons are high surface area solids with rich surface functionality and as a result, find use in a variety of industrial separation processes. The market for activated carbon is already established and growing but there is a huge push to find sustainable alternatives for the raw material used for its production, which is primarily coal. While there exists a significant amount of research on agricultural residues as potential replacements, there is minimal information on using polysaccharides as precursors for the production of activated carbon.

Using the patented PGX process, two separate approaches were employed for the synthesis of activated carbon. The first method relied on the porous network of PGX materials to be maintained during pyrolysis while the second approach used a chemical agent to create porosity during the pyrolysis.

Gas sorption analysis revealed that the PGX structure was not maintained during the pyrolysis stage hence losing all its pore network and extended surface area. Additionally, no significant variation between the PGX and non PGX variants of the chemically activated polymers was observed.

However, it was revealed that the interaction between zinc chloride and pectin produced exceptionally high specific surface area (exceeding 2000 $m^2 g^{-1}$) activated carbon. The produced carbon had a high degree of microporosity (up to 100%) with some flexibility present in tuning the porosity. Elemental analysis revealed the carbon to have high

surface functionality and preliminary adsorption test for removal of heavy metal ions from water ($Pb^{2+}$ and $Cd^{2+}$) showed promising results with the in-house carbon performing better than a representative commercial carbon.

This study relies on statistical methods including multiple design of experiment studies and advanced characterization techniques to analyze the manufacturing process and the properties of carbon in an attempt to find the best conditions for producing activated carbon from polysaccharides.

# Acknowledgements

I would like to express my sincerest gratitude to my supervisors Dr. David Latulippe and Dr. Todd Hoare for giving me the opportunity to work with them. For nearly 24 months I have continuously improved both as a researcher and a human, thanks to their encouragement and support at all times.

I would like to acknowledge Ceapro Inc. and Natural Sciences Engineering Research Council of Canada (NSERC) for financially supporting the project. I would particularly like extend my appreciation to Dr. Bernhard Seifried, and Paul Moquin from Ceapro for their excellent hospitality during my visit to Edmonton.

This project would not have seen the light of the day without the use of so many sophisticated instruments in various labs. I would particularly like to thank the research group of Dr. Charles de Lannoy for getting the BET instrument and allowing me to have unrestricted access to it and helping me to expedite my research. I would also like to thank the research groups of Dr. Hatem Zurob, Dr. Alex Adronov, Dr. Robert Pelton, Dr. Shiping Zhu and Dr. Emily Cranston for allowing me to access their laboratory instruments. I would like to acknowledge Marcia Reid at the Electron Microscope Facility, Chris Butcher at the Canadian Centre for Electron Microscopy, Andrew Kacheff at the University of Waterloo, Xiaogang Li in the department of Material Science and Engineering at McMaster University and Rupesh Pandey at Guelph Chemical Laboratories.

I would like to thank Kelli-anne Johnson for taking the responsibility of routinely travelling to Edmonton and processing the raw materials using the PGX process for everyone involved in this project, I would also like to thank her and Nicola Muzzin for working with me together on this project and providing me with the moral support during all the hard times. I would like to thank all of the group members from the Latulippe research group, without whom the experience would have been much less enjoyable. A special thanks to Reza Pazouki, Amir Kazemi, Shabnam Shoaebargh, Patrick Morkus, Ryan LaRue, and Daniel Osorio for being more than just research mates and sharing the fun during all my failures and constantly encouraging me to deliver better results.

Last, but not the least I would like to thank my mom Shoma Sarkar and dad Dr. P.C Sarkar for their unconditional support and love. It's not easy moving to a new country but hopefully, I made you proud. As a special mention, I would like to thank my girlfriend Karina Kawka for being everything I could have asked for in a partner.

# Table of Contents

# List of Figures

# List of Tables

# List of Acronyms

| | |
|---|---|
| AC | Activated carbon |
| BET | Brunauer–Emmett–Teller |
| CAGR | Compound annual growth rate |
| CNC | Cellulose nano crystal |
| DFT | Density functional theory |
| DI | De-ionized |
| DOE | Design of experiment |
| EDC | Endocrine disrupting compound |
| GAC | Granular activated carbon |
| HMW | High molecular weight |
| IUPAC | International union of pure and applied chemistry |
| LNG | Liquid natural gas |
| MR | Mass ratio |
| MTBE | Methyl tert-butyl ether |
| PAC | Powdered activated carbon |
| PGX | Pressurized Gas Expanded |
| $pH_{ZPC}$ | pH Point of zero charge |
| PV | Pore volume |
| RSS | Residual sum of squares |
| SEM | Scanning electron microscopy |
| SSA | Specific surface area |
| TGA | Thermogravimetric analysis |
| THM | Trihalomethane |
| VOC | Volatile organic carbon |

# CHAPTER 1: Introduction and Literature Review

## 1.1 Introduction

Activated carbon (AC) refers to a broad range of highly porous carbonaceous materials. The pore distribution of these materials can be classified as microporous (pore width < 2 nm), mesoporous (2-50 nm) or macroporous (>50 nm) [1]. This porosity is developed during the controlled thermal decomposition of the parent raw material as part of the production process which results in these materials having extremely large specific surface areas, easily exceeding 1000 $m^2$ $g^{-1}$. In addition to the large internal surface areas, they also have rich surface functionality due to the presence of several heteroatoms on its surface (oxygen, nitrogen) making them ideal materials for use in separation processes.

The primary forms of AC are granular (GAC), powdered (PAC) and pellets and is possible to tune the surface functionality to tailor the intended applications by various process modifications. Some of them include oxidation [2] to modify acidic behavior, sulphurization [3] to improve metal binding capacity, nitrogenation [4] to improve electrochemical nature and impregnation with precious metals for catalytic reactions[5][6]. The flexibility in pore size distribution and possible surface modifications make it of high industrial value. Applications of AC include water purification for removal of contaminants like dyes [7][8], volatile organic matter (VOCs) [9] and heavy metals [10][11]. Gas phase applications include purification of flue gas [12][13]and $CO_2$ capture. Activated carbon has also been used in heterogeneous catalysis for various

organic and inorganic synthesis reactions[14][15]. More recently there has been considerable interest to use it as an adsorbent for storing of natural gas and hydrogen in form of adsorbed natural gas (ANG) [16][17].

The global AC market was worth approximately USD 2.84 billion in 2017, showing a compound annual growth rate (CAGR) of 13.0% between 2012 and 2017, and the market size is estimated to be over USD 6.0 billion by 2023 [18]. Stringent environmental protection laws have increased the demand for AC for application in water treatment and air purification and the demand will only continue to grow. Since coal serves as one of the major raw material for the production of AC [19], even accounting for nearly 64% of the Chinese AC market [18], there exist large amounts of research focusing on finding suitable sustainable alternatives, most of them inclined towards agricultural residues and waste products. The present work focuses on using another class of sustainable materials namely polysaccharides as a potential replacement for coal for the production of AC. The project takes inspiration from the Starbon™ [20] process which has previously used polysaccharides for the production of mesoporous AC. While the Starbon™ process using a gelation technique for creation of the porous network, this work will primarily focus on creating the porous carbon using conventional manufacturing techniques and aims to utilise the advantages offered by the PGX® [21] process. The properties, characterization techniques, production methods and applications of AC, as well as the motivation, uniqueness, and scope of the project are all discussed in detail in the succeeding sections.

## 1.2 History of activated carbon

Activated carbon has been a part of human civilization for thousands of years now. Going back all the way to 1500 B.C there have been documentations of the Egyptians use of "charcoal" to absorb unpleasant odour, cure digestive ailments and for preserving the dead. By 50 A.D, Hippocrates was known to use charcoal for a number of medicinal purposes [22].

It was in the 1700s that major strides were taken in the field of AC. In 1773, chemist Carl Wilhelm Scheele quantified porous carbon by measuring the volume of gases adsorbed by the material. The major discovery, however, was in 1794, when a sugar refinery found that carbon could be used as a decoloring agent. This revolutionized the sugar industry, by producing more white and appealing sugar. Within the next decade, all of Europe was using charcoal to decolor sugar. After the AC process was developed around 1820, there were widespread studies on its use as an antidote for poison treatment [22].

In 1862, Frederick Lipscombe helped pave the way for commercial applications of AC by using the material to purify potable water. Physicist Heinrich Kayser, coined the term "adsorption" to describe charcoal's ability to uptake gases in 1881 [22].

Activated carbon was first produced on an industrial scale at the beginning of the 20$^{th}$ century. During the First World War AC was used in gas masks to protect from poison gas. Throughout the 20th century and moving into the 21$^{st}$ century, AC has found widespread use across multiple industries in form of water purification, decolorizing, air purification and medicinal purposes.

## 1.3 Structure and properties of activated carbon

The heterogeneous nature, as well as the vastness in possible variations of AC, make it difficult to completely understand its structure, although some similarities exist in the overall morphology of the many ACs in the market. The structure of AC can be visualized as a random distribution of organized graphitic crystallites mixed with a disorganized amorphous phase comprising of complex aromatics and aliphatics. These fractured graphitic crystallites are randomly oriented, extensively interconnected and this anisotropic crystallite alignment leads to the presence of voids [23]. Unlike the ordered hexagonal rings of graphite that stack on top of each other, the rings in AC are randomly oriented and lack any directional relationship (**Fig. 1**) [24]. The heteroatoms (oxygen, sulphur, nitrogen, phosphorus) are mostly located at the edge of these broken graphite rings, allowing the possibility of many reactions.

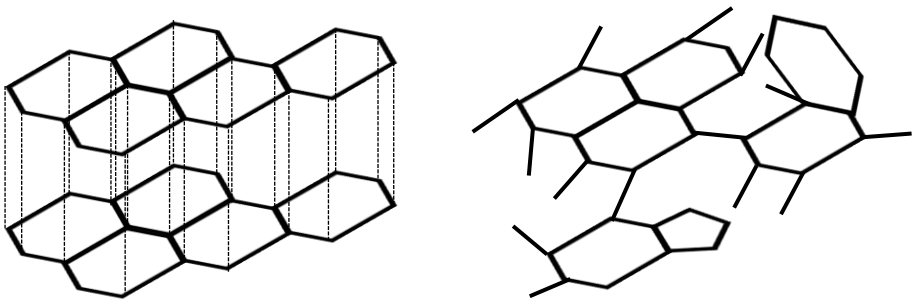

**Figure 1.** Structure of graphite (left) and AC (right). While graphite has an organized structure with hexagonal sheets stacked on top of each other, AC has more of a distorted structure with the sheets randomly oriented.

Since AC mainly functions through adsorption, which involves the adhesion of adsorbate molecules on the surface of the carbon, a large specific surface area (SSA) is one of the most important properties used for characterization of AC. The adsorption process occurs

due to the unbalanced forces that exist on carbon atoms at the surface. Since adsorption is a spontaneous process (**$\Delta G < 0$**), and surface adsorption proceeds with a decrease in entropy (**$\Delta S < 0$**), the resultant means that adsorption must always be an exothermic process (**$\Delta H < 0$**) [24].

This adsorption behavior can be classified as physical or chemical adsorption. Physical adsorption takes place via weak van der Waals forces, as well as hydrogen bonding and the process is usually reversible. Chemical adsorption usually refers to the adhesion of molecules via permanent bonds (covalent or ionic) and are irreversible. The adsorptive behavior of AC in aqueous solution is influenced by temperature, pH of the solution, the chemical nature of species and its concentration, and the pore distribution of the AC. The versatile nature of AC allows it to interact with various molecules. However, due to the same reason, it is extremely difficult to identify a single mechanism by which this adsorption process takes place. Due to the non polar nature of AC, it adsorbs organic compounds preferentially in comparison to polar inorganic species [24].

While high surface area and well defined pore size distribution are the primary factors that affect the adsorption behavior of adsorbate molecules on the surface of AC, the nature and amount of surface groups present must also be accounted for to understand the adsorption behavior [23]. Among these oxygen containing surface groups are the most commonly found. **Fig. 2** summarizes the most common types of surface groups that may be found on AC.

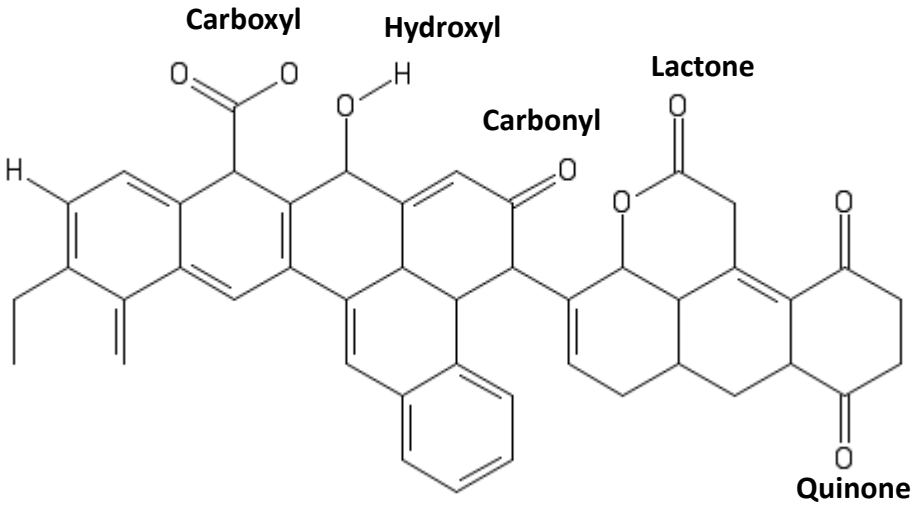


**Figure 2.** Some common oxygenated functional groups found on AC.

Although the functional groups represent only a small fraction of the total surface area, a small variation in the chemical nature of the AC can produce significant changes in its adsorption capacity. Activated Carbon, in general, is hydrophobic in nature, however, the presence of polar oxygenated groups can increase the hydrophilicity as the water molecules can form hydrogen bonds with oxygen atoms of the surface groups. These surface groups also influence the acidic and basic nature of the AC.

For aqueous based adsorption process another important factor that needs to be considered is the pH of the solution with respect to the point of zero charge of the AC. At the point of zero charge, the oxygenated functional groups of the AC are in un-dissociated form and do not contribute to the pH of the solution. However, if the pH > $pH_{ZPC}$, acidic functionalities will dissociate, releasing protons into the medium and leaving a negatively

charged surface on the AC. On the other hand, if the pH < $pH_{ZPC}$, basic sites combine with protons from the medium to leave a positively charged surface [23].

## 1.4 Manufacturing of activated carbon

### 1.4.1 Raw materials

Activated carbon can be produced from any material rich in carbon, as a result, there exist plenty of possible raw materials such as wood, lignocellulosic biomass, peat, lignite and different grades of coal that can be used to make AC. Since the manufacturing process involves the removal of volatile matter from the raw material, the higher the fixed carbon content the higher is the yield [24]. As a result, one of the advantages of coal is their relatively low volatile content and, hence, their high yields.

**Table 1.** The fixed carbon content of common raw materials used for the production of AC [24].

| Material | Approximate carbon content (%) |
|---|---|
| Soft wood | 40 |
| Hard wood | 40 |
| Coconut shell | 40 |
| Lignite | 60 |
| Bituminous coal | 75 |
| Anthracite coal | 90 |

### 1.4.2 Production process

The production routes can be classified into two major categories, physical and chemical activation. Physical activation is usually a two-step process that involves pyrolyzing the precursor at a low temperature of 400-500 $^{o}$C **(carbonization step)** followed by

activation with steam or $CO_2$ at higher temperatures of 800-1000 $^oC$ **(activation step)** [25].

Chemical activation is a one-step process with both carbonization and activation taking place simultaneously, during which the precursor is mixed with an activating agent, usually, a strong dehydrating agent such as $ZnCl_2$, $H_3PO_4$ or KOH followed by pyrolyzing at relatively low temperatures (400-600 $^oC$).

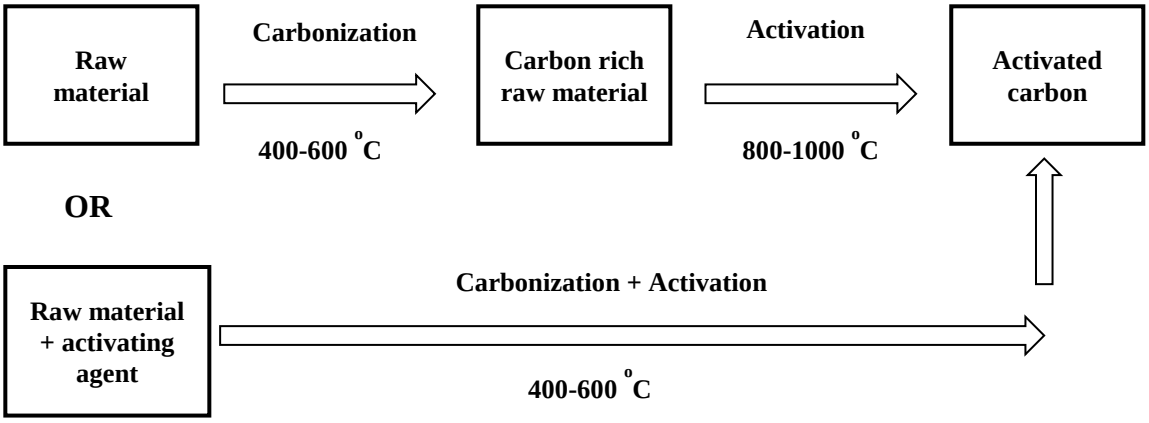


**Figure 3.** The production process for AC. Physical activation (top) is a two step process, whereas chemical activation (bottom) is a one step process with carbonization and activation taking place simultaneously.

### 1.4.2.1 Carbonization

During the process of carbonization, the carbon atoms rearrange themselves into graphite like rings and the resultant product has an increased fixed carbon content [25]. During this step, a series of decomposition and rearrangement reactions are initiated in the parent polymeric network. Free radicals are generated and considerable strain energy is introduced in to the lattice. The polymeric structure, on pyrolysis, loses volatiles in form of small molecules like $H_2O$ and CO as well as large molecules in form of hydrocarbons.

These evolutions do not occur at single decomposition temperature but over a range of temperature. Consequentially, the newly created exo-skeleton has a composition of higher C/H and C/O ratios due to the preferential loss of hydrogen and oxygen [26].

#### 1.4.2.2 Activation

The internal surface area and porosity of the AC are developed during the second or the activation step. Activation is carried out to enhance the diameter and volume of the pores, which are created during the carbonization process. Activation is known to take place in two stages [26]. In the first stage, the disorganized carbon lattice is burnt out preferentially and the closed and clogged pores between the crystallites are freed leading to the formation of primary microporous structure. During the second stage, widening of the existing pores and leading to the formation of meso and macro pores are observed.

The activating agent can be an oxidising gas ($O_2$, steam, $CO_2$,) as in the case of physical activation or a chemical agent like in the case of chemical activation. The chemical activating agents act as dehydrating agents, which influence the controlled thermal decomposition of the precursor and inhibit tar formation. They are also known to decrease the formation of hydrocarbons thereby improving the yield of carbon. During chemical activation, the chemical agent attacks the polymer structure of the precursor and water is eliminated leading to increased cross linking and aromatization in the parent polymer network. The pore size distribution of the AC depends on the mass ratio of the chemical agent used, as a result, the higher the ratio, the higher the development of meso and macroporosity [26].

While both mechanisms (physical or chemical) produce AC with a high degree of porosity and increased surface areas, the ACs differ greatly with respect to physical and chemical properties. Due to lower temperature requirements for the chemical process, the yield is reportedly higher as there is reduced carbon burn off. However, due to the low temperatures used the chemically AC lack the high degree of graphitization compared to the physically ACs. Since each method has its own merits and demerits, a hybrid process that includes low temperature chemical activation followed by high temperature physical activation has been suggested in the past [25].

## 1.5 Techniques for characterization of activated carbon

Activated carbons are complex heterogeneous materials that are difficult to characterize completely based on a single chemical or physical analysis technique. They differ in size, shape, surface functionality and porosity. The variability comes from both the starting material (raw material) and the production route (chemical or physical) employed. Even so, standard methods of characterization specifically related to the pore size distribution and surface area measurements have been established to assess the adsorption potentials and compare different ACs. A few techniques that allow us to study the surface and pore size distribution of AC are described below.

### 1.5.1 Scanning Electron Microscopy (SEM)

This technique allows us to study the topography of the AC. The exteriors which usually contain large pores (meso and macro) can be detected visually by the instrument and provide us with an insight on the transport mechanics that might take place when the AC

is used for adsorption. It is these pores that allow the transport of the adsorbate molecules from the bulk of the solution to the interiors of the pores where the adsorption occurs. Although very rudimentary, this technique is still widely used to visually detect the topographical changes that take place during the production process by comparing the SEM images of the raw material to the final product.

### 1.5.2 Mercury porosimetry

This method is widely used for characterization of porous powders as it allows the determination of pore size distribution. Mercury is a non-wetting liquid and as a result, will not penetrate inside any pores under capillary action. However, it is possible to force inside by the application of external force and the pressure required is inversely proportional to the size of pores. The technique involves progressive intrusion of mercury into a porous solid with increasing pressure. The pore size and volume distribution for cylindrical pores are then generated using the Washburn equation [27]. As the required pressure increases with a decrease in pore size the method is typically not suitable for detection of micro and ultra micropores as the applied high pressures can cause the pore walls to collapse, resulting in erroneous measurements.

### 1.5.3 Gas sorption

This measurement technique is by far the most widely recognised technique for the characterization of AC and porous materials in general. Measurement typically involves characterizing the material using the adsorption and desorption isotherms data of a non reactive gas on the adsorbent surface. In this technique, a known amount of gas is fed to a

sample bulb at constant adsorption temperature. Adsorption of the gas on to the sample occurs, and the pressure in the sample cell volume continues to fall until the adsorbate and the adsorbent are in equilibrium. The amount of adsorbate at the equilibrium pressure is the difference between the amount of gas admitted and the amount of adsorptive remaining in the gas phase [28]. **Fig. 4** represents the various stages of the gas sorption process as the pressure inside the sample cell is increased. Nitrogen is the most widely used gas and the sorption is done at 77 K. It is, however, possible to generate these isotherms using other gas molecules like argon (77 K), krypton (77 K), xenon (77 K), and carbon dioxide (195 K).

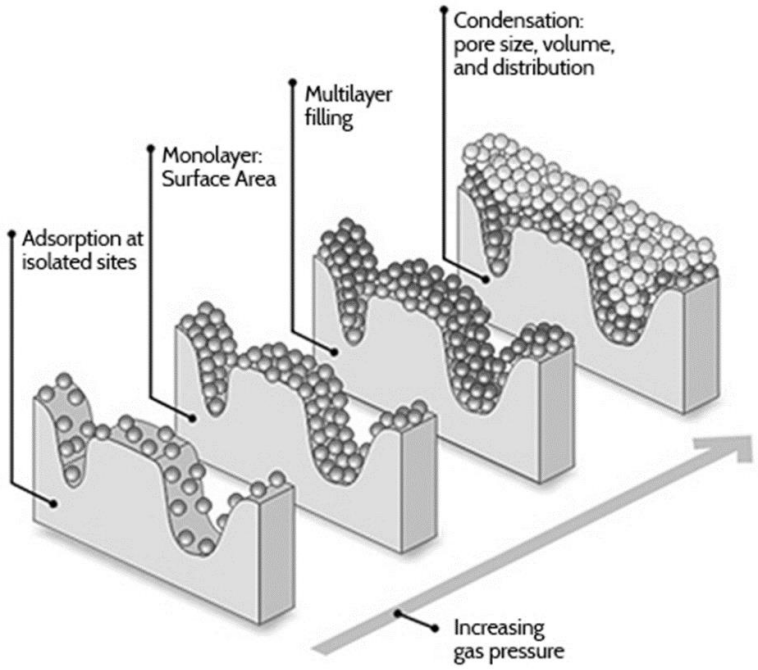


**Figure 4.** Schematic representing the gas sorption process. The surface area calculation is done at the monolayer coverage (P/Po <0.35), while the pore volume and size distribution calculations are done at relative pressures close to unity [29].

### 1.5.3.1 Types of sorption isotherms and hysteresis loops

The shape of the sorption isotherm is the first indicator of the type of pore structure of the AC. The different types of isotherms are generated because of the different nature of interaction that takes place between the adsorbent and the adsorbate in the different pore regimes (micro, meso or macro). **Fig. 5** shows the different type of physisorption isotherm curves based on IUPAC classification [30]

*Type I* isotherms are characteristic of a microporous solid. For these materials, the amount of gas that can be adsorbed approaches a limiting value which is governed by accessible micropore volume. Type I (a) correspond to materials having mainly narrow micropores and Type I (b) with a slightly broader pore size distribution with narrow mesopores (< 2.5 nm).

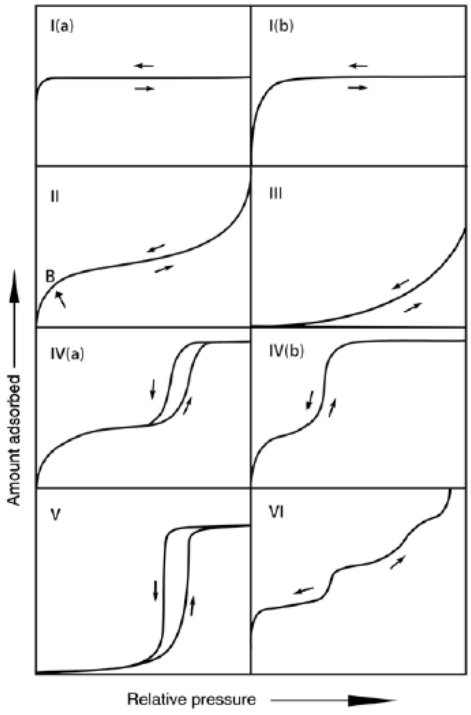


**Figure 5.** IUPAC classification of gas sorption isotherms [30]

*Type II* isotherms correspond to non porous or macroporous adsorbents. The shape is due to unrestricted multilayer adsorption at higher relative pressures. Point B corresponds to completion of monolayer coverage.

*Type III* isotherms have no point B, hence no identifiable monolayer coverage. The adsorbent-adsorbate interactions are relatively weak.

*Type IV* isotherms are given by mesoporous solids. In these solids, the initial monolayer-multilayer adsorption is followed by pore condensation. Type IV (a) materials a hysteresis loop is observed. Hysteresis is observed for pore width wider than 4 nm. For mesopores with smaller pore width, Type IV (b) isotherms are observed.

*Type V* isotherms are observed for water adsorption on hydrophobic microporous or mesoporous materials.

*Type VI* isotherms are indicative of layer by layer adsorption on a highly uniform, non porous solid.

As previously described, a distinct hysteresis loop is observed for mesoporous materials. Many different types of hysteresis lops have been reported but the most important ones are presented in **Fig. 6.**

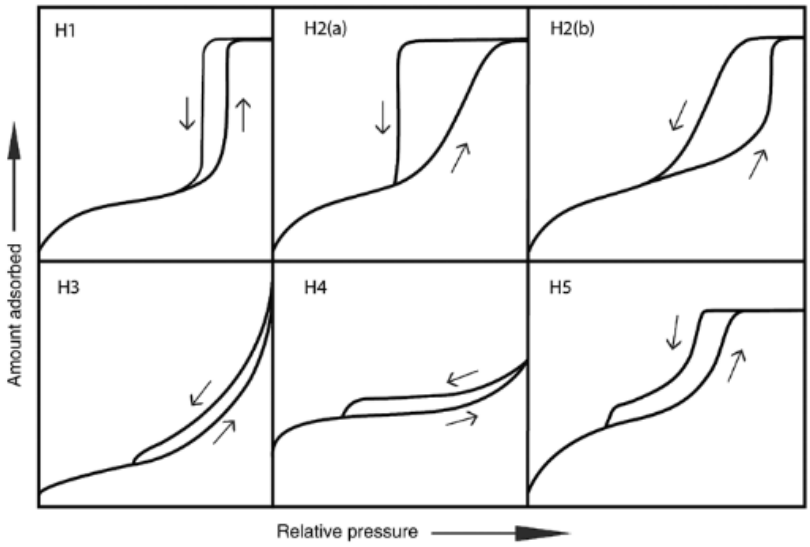


**Figure 6.** IUPAC classification of gas sorption hysteresis loops [30]

*Type H1* loop is found in materials which exhibit a narrow range of uniform mesopores, Examples include templated silica and ordered mesoporous carbons.

*Type H2* is given by materials have more complex pore structures. H2 (a) loops are given by many silica gels, some porous glasses as well as some ordered mesoporous materials.

*Type H3* loop is given by non-rigid aggregates of plate-like particles but also if the pore network consists of macropores which are not completely filled with pore condensate.

*Type H4* is a composite of Types I and II. H4 loops are often found with aggregated crystals of zeolites, some mesoporous zeolites, and micro-mesoporous carbons.

*Type H5* loop is unusual and has been noticed in some hexagonal templated silica materials.

### 1.5.3.2 Determination of surface area: BET method

The Brunauer–Emmett–Teller (BET) method continues to be the most widely used technique for determination of surface area of porous solids. The theory is an extension of the Langmuir theory, with the same basic assumptions:

- The surface of the material is homogeneous, with no preferential adsorption sites.
- No intermolecular (lateral) interactions take place between adsorbed molecules
- Gas molecules adsorb on solid in layers infinitely
- Langmuir theory can be applied to each layer

The generalised BET equation for gas adsorption can be expressed as:

$$W = \frac{W_m \times C}{(P_o - P)[1 + (C - 1)\left(\frac{P}{P_o}\right)]}$$

Where W is the weight of gas adsorbed at a relative pressure P/Po and $W_m$ is the weight of adsorbate for monolayer coverage. C is the BET constant and is related to the energy of adsorption of the monolayer. When the value of C is at least 80, the point B in an isotherm is easily identifiable indicating completion of the monolayer. At values of B ~50, point B cannot be identified as a single point on the isotherm and there is an overlap of monolayer-multilayer adsorption. When C is < 2, the isotherm is type III or type V and BET method is not applicable. A high value of C (> 150) is associated with the filling of high energy site or filling of micropore [28].

The linear form of the equation can be written by rearranging the terms:

$$\frac{1}{W[\left(\frac{P_o}{P}-1\right)]}=\frac{1}{W_mC}+\frac{C-1}{W_mC}(\frac{P}{P_o})$$

The BET equation is only linear in a limited range of relative pressure (0.05-0.35). This linear range is known to shift to lower relative pressures for microporous materials. A standard multipoint BET procedure requires a minimum of 3 points in appropriate relative pressure range. Using the knowledge of the molecular cross sectional area ($A_{cs}$) of the adsorbate gas, the total surface area of the solid can then be found out using:

$$S_{Total}=\frac{W_m\times N\times A_{cs}}{M}$$

Where N is Avogadro's number ($6.022x10^{23}$ molecules/mol) and M is the molecular weight of the adsorbate. The value of $A_{cs}$ for nitrogen is $16Å^2$. The SSA of the solid can then be calculated from the sample weight (W) used:

$$S_{BET}=\frac{S_t}{W}$$

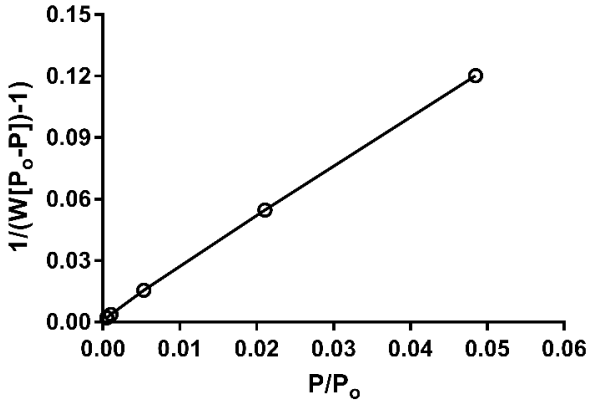


**Figure 7.** A typical BET plot. The linear range of the equation, in this case, has shifted to lower relative pressures (<0.1) indicating a high degree of microporosity. The particular plot is for zinc chloride AC from pectin.

While the BET equation while is widely used and applicable for nonporous and some mesoporous materials, certain precautions need to be taken for its applicability to microporous materials. It may be impossible to separate monolayer adsorption from micropore filling for such materials and the linear range for the BET equation may be difficult to determine as the monolayer coverage takes place at much lower relative pressures (<0.1). As a result, the values of surface areas obtained maybe underestimated. A few precautions that help in avoiding such problems are underlined below:

- The quantity C should be positive
- The application of the BET equation should be restricted to the range where the term $W(1-P/P_o)$ continuously increases with $P/P_o$
- The $P/P_o$ value corresponding to $W_m$ should be within the selected BET range.

As a final precaution, the values of $W_m$ and surface area obtained can be reported as apparent BET surface area which may not represent the true monolayer coverage.

For the present work which utilises the Autosorb iQ and Quadrasorb software for determination of BET surface area, the software has an inbuilt feature called the "Micropore BET assistant" that helps in determining the valid linear BET range for accurate surface area calculation [31].

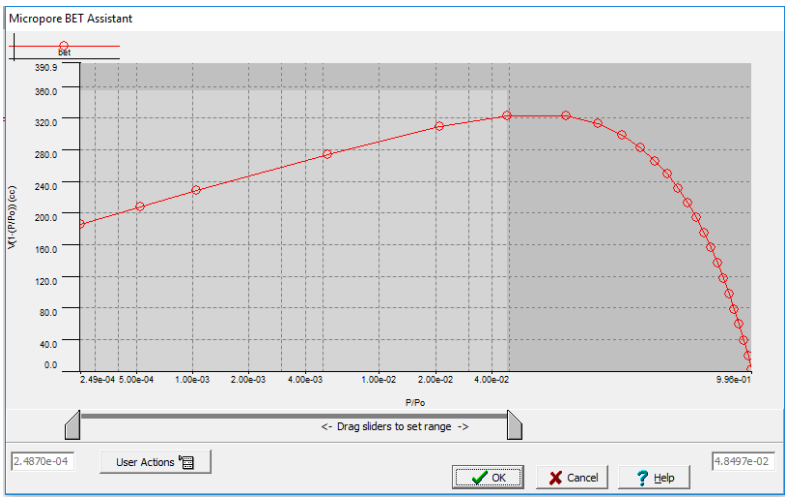


**Figure 8**. Screenshot of the micropore BET assistant available in *Autosorb iQ* software. The highlighted region, where the curve is straight represents the linear range of the BET equation

### 1.5.3.3 Determination of pore volume and pore size distribution

#### Pore Volume

The total pore volume (PV) calculations are based on the amount of vapor adsorbed at a relative pressure close to unity, assuming that the pores are then completely filled with liquid adsorbate. If the solid contains no macropores, the isotherm will remain nearly horizontal over a range of $P/P_o$ approaching unity and the pore volume is well defined. However, in the presence of macropores, the isotherm rises rapidly near $P/P_0 = 1$ and the total pore volume has to be estimated by other methods (like mercury porosimetry). The volume of nitrogen adsorbed ($V_{ads}$) can then be converted to the volume of liquid nitrogen ($V_{liq}$) contained in the pores using the equation:

$$V_{liq} = \frac{P_a \times V_{ads} \times V_m}{RT}$$

Where $P_a$ and T are ambient pressure and temperature, respectively, and $V_m$ is the molar volume of the liquid adsorbate (34.7 $cm^3\,mol^{-1}$ for nitrogen).

The average pore radius assuming cylindrical pore geometry can be calculated as:

$$r_p = \frac{2 \times V_{liq}}{S_{BET}}$$

**Pore Size Distribution (mesopores)**

The pore size distribution for mesoporous solids can be calculated using several models that make use of the Kelvin equation for calculating the pore radius. Popular computational models include the Barrett, Joyner, and Halenda [32] and the Dollimore and Heal models.

**Pore Size Distribution (micropore)**

A number of different methods have been proposed for the analysis of pore size distribution of microporous material. They can be divided into macroscopic procedures and those based on statistical mechanics. Popular models include empirical methods like the V-t method, Dubinin-Radushkevich method, Horvath-Kawazoe method and Saito-Foley method [28]. However, these classical models do not give a realistic description of the filling of micropores leading to an underestimation of pore size. In order to achieve a more realistic description microscopic theories, which describe the sorption and phase behavior of fluids in narrow pores on a molecular level. Models such as the Density Functional Theory (DFT) or Monte Carlo simulation provide a much more accurate approach for pore size analysis and bridge the gap between the molecular level and macroscopic approaches [33] [34].

## 1.6 Applications of activated carbon

As previously mentioned AC finds its use in a variety of applications, some of which are discussed below.

### 1.6.1 Water treatment

One of the major markets for AC is in municipal drinking water treatment. GAC is typically employed for removal of taste and odour, pesticides, color, Trihalomethanes (THMs) and other micropollutants. Activated carbon is also used for home water treatment where they are employed at the point of use inside jugs or at the tap. Silver impregnated ACs are used frequently used to improve bacteriostatic properties. AC is widely used for treating industrial wastewater for removal of organic compounds like $H_2S$, Methyl tert-butyl ether (MTBE), Bisphenol A (BPA) and numerous endocrine disrupting compounds (EDC). It is also used for treating landfill leachate and used in ground water remediation [35].

### 1.6.2 Air purification

Activated carbon is routinely employed for removal of volatile organic compounds (VOC), siloxanes from biogas production facilities and $H_2S$ and mercaptans from sewage treatment works and industrial effluent facilities. PAC is used for the treatment of flue gas generated from incinerators of municipal solid waste, sewage sludge or medical waste and efficiently remove dioxins and heavy metals like mercury and cadmium. Activated

carbon is widely used for mercury scrubbing generated from coal fire power plant, cement and steel industries [35].

### 1.6.3 Industrial processes

Activated carbon is used in decolourisation applications for colour removal from liquid chemicals like liquid natural gas (LNG), synthetic oils, and plasticizers. It is used for solvent purification like recirculating amine in amine scrubbers, removal of mercury during the Chloralkali process and removal of metal finishing residues and trace organics in electroplating industries. It finds its use in hydrogen purification during pressure swing adsorption [35].

Activated carbon is used in the food and beverage industries for decolorisation and purification applications. It finds its use in decolourising cane and beet sugar syrups, dextrose, fructose, and other food products, purify carbon dioxide for use in carbonated drinks. Remove unwanted taste/odour or colour compounds from alcoholic beverages and even decaffeinate tea and coffee [35].

### 1.6.4 Miscellaneous applications

Activated carbon is used by mining industry for recovery of gold, precious rare earth metals from ore, waste and reclaim streams. It is used for purification of pharmaceuticals for colour and protein removal. Activated carbon finds its use in personal protective equipment in form of respirator filters [35].

The massive range of applications means there exist wide variations in the types of AC available in the market, a critical feature differentiating the various ACs is the pore size distribution of the carbon. A simplified table highlighting the pore size requirement of major applications is listed in **Table 2.**

**Table 2** Pore size requirement for various applications of AC

| Application | Pore Size Requirement |
|---|---|
| Water Treatment | Distribution of micro and mesopores **(1-10nm)** |
| Gas Purification | Narrow distribution of micropores **(0-2nm)** |
| Catalysis | Mesopores **(>2 nm)** |
| Supercapacitors | Micro and ultra micropores **(0.7-1nm)** |
| Gas Storage | Micro and ultra micropores |

## 1.7 Project motivation and previous work

### 1.7.1 Demand for activated carbon and coal as the raw material

The wide range of possible applications and the possibility of surface modifications make AC an extremely valuable material for both the industry and researchers. As a result, the demand for AC is constantly growing. The global demand for AC was 1.65 million tons in 2016 with a CAGR of 6.3 % in the period 2012-2016 [36]. Coal continues to be the major source of raw material for the production of AC due to its ease of availability and low cost. However, as with all other fossil fuels, coal too is an exhaustible resource and at

the current rate of production is estimated to last around only 150 years [37]. With global increase in awareness of the health implications of working with coal which inherently contains toxic trace metals, like mercury [38] combined with environmental protection acts to provide cleaner air and water raising the demand for AC , the situation has garnered significant interest of researcher for finding sustainable and greener alternatives and there exists huge potential to break into the market with a suitable replacement. The possible potential alternatives are discussed in further sections.

### 1.7.2 Agricultural residues as alternatives to coal

As a consequence of the need to find sustainable alternatives to coal, a significant amount of research has been done on the use of agricultural residues as raw material for the production of AC. A wide range of such materials like seeds, shells, straws, and peels have been tested using both chemical and physical methods of activation. A short summary of the process conditions and specific surface area for numerous agricultural residues is listed in **Table 3.**

The cheap availability of agricultural residues would seem to make them a viable choice for production of AC. However, as it can be observed from **Table 3** that while there is some promise in some cases with regards to the specific surface areas obtained, there exists massive variation among different raw materials. This is due to the inherent heterogeneous nature of the precursor and complexity in chemical compositions among different starting material.

Typical SSAs are limited to < 1000 $m^2$ $g^{-1}$ for most precursors and a minimal emphasis is given to the pore size distribution in these studies. While higher SSA, exceeding 1500 $m^2$ $g^{-1}$ have been obtained, for example, AC from fox nut shells was reported to have a SSA exceeding 2000 $m^2$ $g^{-1}$ via $H_3PO_4$ activation at a temperature of 700$^oC$ and impregnation ratio of 1.5 [39]. Such reports are few and typically to obtain such high SSA values severe process conditions are required, with temperatures exceeding 700$^oC$ or large quantities of the activating agent being used.

Apart from the heterogeneous nature of the materials, many of the starting materials are geographically localized and as a result, lack the availability/ accessibility, unlike coal. The heterogeneous nature also poses a challenge to establish consistent process conditions at the manufacturing stage. These challenges have prompted the researchers to look beyond just agricultural residues as a potential replacement for coal for the manufacture of AC.

**Table 3** Brief summary of previous work on using agricultural residues as precursors for the production of AC

| Sl. | Material | Method of production | Activating agent | Process conditions | SSA ($m^2$ $g^{-1}$) | Reference |
|---|---|---|---|---|---|---|
| 1 | Pistachio nutshell | Physical | $CO_2$ | 500°C | 778 | [40] |
| 2 | Almond shells | Physical | $CO_2$ | 850°C | 1000-1200 | [41] |
| 3 | Corn hull | Physical | $CO_2$ | 700-800°C | 900-1000 | [42] |
| 4 | Corn stover | | | | 400-600 | |
| 5 | Oak wood waste | | | | 600-900 | |
| 6 | Oat hulls | Physical | Steam | 800°C | 300-600 | [43] |
| 7 | Corn stover | Physical | | | 300-400 | |
| 8 | Rice straw | Chemical | KOH | 500-900°C | 300-900 | [44] |
| 9 | Cassava peel | Chemical | KOH | 450-750°C | 900-1300 | [45] |
| 10 | Olive stone | Chemical | $H_3PO_4$ | 500°C | 300-1200 | [46] |
| 11 | Macadamia nutshell | Chemical | $ZnCl_2$ | 500-800°C | 1500-1800 | [47] |
| 12 | Corn cob | Chemical | $ZnCl_2$ | 400-800°C | 400-900 | [48] |
| 13 | Apricot stone | Chemical + Physical | $H_2SO_4$ + Steam | 600°C ($H_2SO_4$) + 800°C (Steam ) | 1190 | [49] |
| 14 | Grape seeds | | | | 497 | |
| 15 | Rice Husk | Chemical + Physical | $ZnCl_2$ + $CO_2$ | 600°C ($ZnCl_2$) + 600°C ($CO_2$) | 200-500 | [50] |

### 1.7.3 Polysaccharides as potential alternatives

The search for a suitable alternative to coal for AC production is an ongoing process and another class of materials that may be a strong choice are polysaccharides. Polysaccharides are polymeric carbohydrate molecules composed of long chains of monosaccharide units bound together by glycocidic linkages. Most commonly known polysaccharides include starch, pectin, cellulose, and chitin. Other polysaccharides include laminarin, chrysolaminarin, xylan, arabinoxylan, mannan, fucoidan, and galactomannan. All of the polysaccharides are naturally abundant bio-polymers that are extracted from biomass. Given their known chemistry, it might be possible to control the pore size distribution or perform any pre/post manufacture modifications that ACs offer.

Polysaccharides have already found profound usage in industries. Starch finds its major application in the food industry while paper making continues to be its largest non food industrial application. It also finds usage in textile and adhesive industry. Pectin is used as a thickening agent and stabilizer in the food industry and even finds use in the medical and cosmetic industry. Cellulose which is the most abundant organic polymer on earth is a major raw material in the pulp and paper industry. Due to their known chemistry, ease of availability, sustainable nature and the ability to be produced on an industrial scale, they have garnered significant interest from the research community for various applications. Chemically modified starch has found usage in form of adsorbents [51] while pectin has been used as flocculants in the past [52]. Cellulose in form of nanocrystals (CNCs) has the potential to be used as nanocomposites[53] and adsorbent[54].

There has been developing an interest in using these materials for the production of porous carbon as well. Starting with starch, researchers at the University of York (United Kingdom) have tested a wide range of polysaccharides (starch, pectin and aliginic acid) for the production of mesoporous carbon using their patented Starbon™ technique. In this method, the native polysaccharide is gelatinized by heating in water. The resultant gel is then cooled for 1-2 days. This is followed by a solvent exchange of water with ethanol to yield a porous aerogel. The porous block is then carbonized to yield a porous carbon [20]. The materials obtained have SSA in the range of 200-600 $m^2 g^{-1}$ and are highly mesoporous. The process schematic is presented in **Fig. 9**

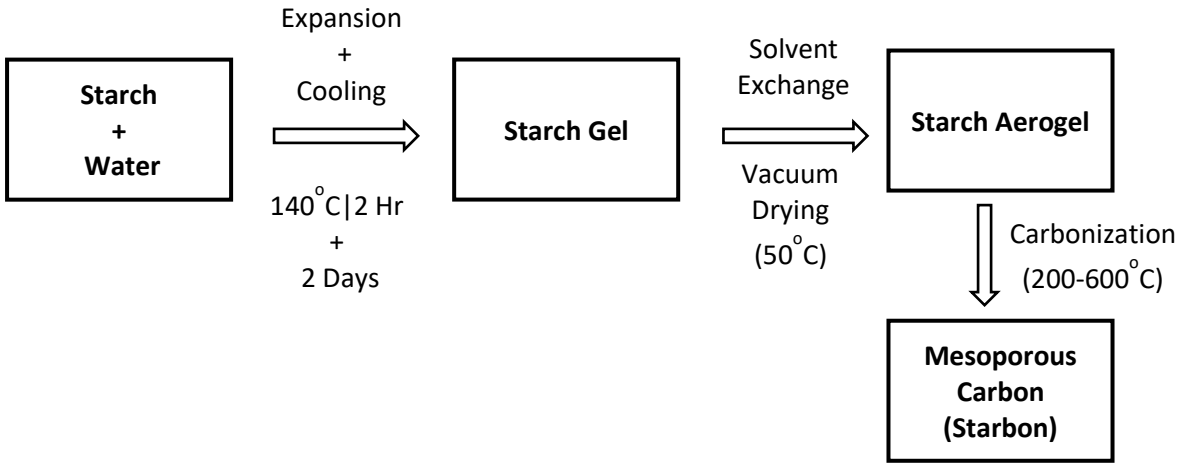


**Figure 9.** Schematic representation of the Starbon™ Process

The Starbon™ process is evidence that it is indeed possible to produce AC using polysaccharides. However, the efficacy of these materials to be used as precursors for the production of AC using conventional techniques (physical or chemical activation) is yet to be established.

Taking inspiration from the Starbon process, it was proposed that there is the possibility of using the patented PGX process for creating porous carbon. Our research partner Ceapro Inc. owns a patented technology known as Pressurized Gas Expanded process or PGX [21] through which they are able to dry high molecular weight (HMW) bio-polymers resulting in high surface area final products. These materials have found usage in various applications and it was suggested that they might also have possible use as raw materials for the production of porous carbon materials. Taking into the disadvantages of coal and short comings of agricultural residues as potential replacements combined with the success of the Starbon process and the potential of PGX processed polymers as sustainable alternatives, an attempt was made to produce AC from PGX processed polysaccharides.

## 1.8 The Pressurized Gas Expanded (PGX) Technology

The PGX process was invented by Dr. Feral Temelli (Professor at the Department of Agricultural, Food & Nutritional Science, University of Alberta) and Dr. Bernhard Seifried, the Engineering Research and Technology Director at Ceapro [55]. It is a novel spray drying technology that utilises supercritical carbon dioxide (S-$CO_2$) and ethanol (EtOH) to precipitate out water soluble bio-polymers leaving behind a dry, highly porous final product. The final form of the bio-polymer can be in form of fine powders, micro fibrils, fine granules or coarse granules.

The PGX Process (**Fig. 10**) utilises the concept of supercritical fluid drying along with gas antisolvent technique to dry HMW water soluble biopolymers. The solvent used is water and the antisolvent is a mixture of supercritical carbon dioxide and ethanol. Under the supercritical condition, $CO_2$ behaves both as a liquid having a high density

(like a liquid) and a gas by expanding to occupy all the space inside a closed vessel. The PGX process is operated at moderate conditions of 100 bar and 40°C. Under these conditions, ethanol is completely miscible in S-$CO_2$ and forms a gas expanded liquid.

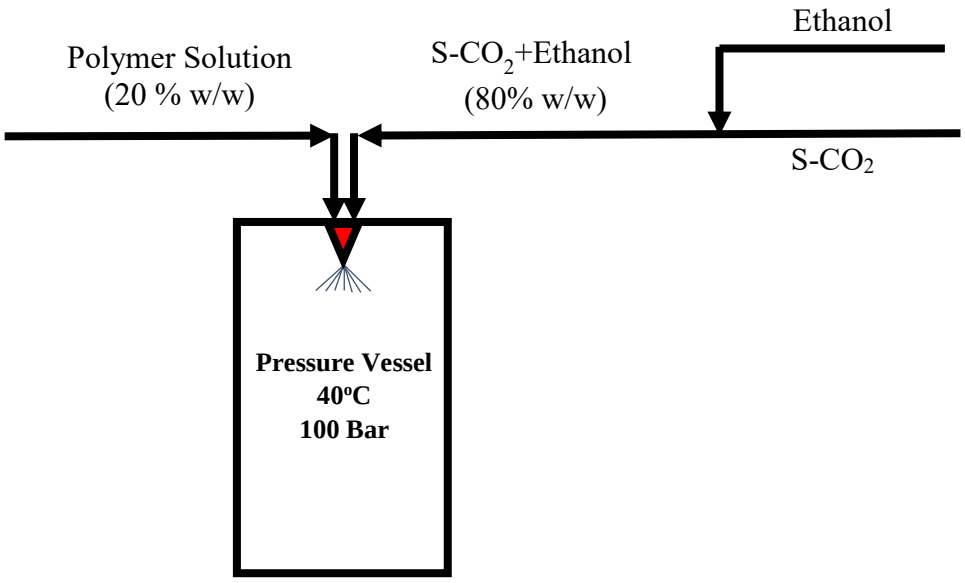


**Figure 10.** Schematic representation of the PGX process

This mixture is pumped through one line, while the aqueous solution of polymer is pumped through a separate line. The two lines mix together inside a co-axial nozzle before entering the vessel. Under the operating conditions, water is completely soluble in the S-$CO_2$-EtOH system, which acts as a solvent for water. At the same time, S-$CO_2$-EtOH acts as an antisolvent for the solute (polymer) present in water, as a result of which the polymer rapidly precipitates out. During precipitation, the polymer is dried, purified and takes its characteristic morphological shape, which can be in form of granules, fibrils or microbeads. The vessel is then pumped with S-$CO_2$-EtOH mixture to pump out all of the water, which is then followed by pumping the vessel

with S-$CO_2$ to pump out EtOH. The vessel is then de-pressurised to obtain the dried polymer.

**Figure 11.** Photograph comparing the same mass of pectin before and after the PGX process

Due to the inherent advantages offered by the process, some applications of the PGX process include:

- Dry aqueous solutions or dispersions of HMW polymers (Polysaccharides or carbohydrates).
- Purification of biopolymers during the drying and precipitation of the polymer.
- Micronize the polymer to a matrix of highly porous fibrils or particles having nano-scale features
- Functionalize polymers and form nanocomposites by mixing of polymer solutions prior to PGX processing.
- Impregnation of the polymer with thermo-sensitive bioactives to improve hydrophilicity and solubility prior to PGX processing.
- Extraction of bioactives from fermentation slurry [56].

For the purpose of this research, it was assumed that due to the porous nature of the PGX processed polymers, that allow them to have high surface areas as well as due to the green nature of the precursors used it is possible to produce porous carbon materials for the purpose of water treatment, gas purification or catalytic applications making it a sustainable and environmentally friendly process.

## 1.9 Project scope

The uniqueness of the PGX process combined with the limited research data available on the use of polysaccharides as raw materials for the manufacture of AC provided the opportunity to explore the vastly untouched research field. The project aims to utilise the advantages offered by polysaccharides combined with the PGX process to successfully make commercial grade AC. The primary focus of the project will be to compare the AC produced from PGX processed polymers to the unprocessed ones. Gas sorption (specific surface area) and SEM (surface morphology) analysis would be used as the primary characterization techniques. Once a suitable material and process conditions have been identified, the project aims to comprehensively characterize the produced carbon for the purpose of being used as a potential adsorbent for water purification.

# CHAPTER 2: Activated carbon from PGX processed polymers

## 2.1 Introduction

The usual routes for the production of AC as discussed earlier include the physical activation and chemical activation methods. Briefly, in these methods, the precursor is first carbonized which increases the carbon content of the material followed by an activation step that leads to the creation of the pore structure of the AC. These two steps can be separate as in the case of physical activation or take place simultaneously as in the case of chemical activation. Finally, the raw material and the choice of production route determine the final pore structure of the AC [25]. There are however other ways of producing porous carbon materials. The Starbon™ process as previously outlined utilises the inherent self assembling nature of polysaccharides in aqueous solution to create mesoporous pore network via gelation mechanism followed by carbonization [57] to produce porous carbon. Taking inspiration from the Starbon™ process an attempt was made to produce porous carbon materials using the patented PGX® process.

The PGX processed polymers have shown to have high surface areas compared to unprocessed polymers with a developed pore structure. For the present study, two different polymers, corn starch, and pectin were chosen for the production of AC due to their wide abundance in nature. Both these material are in form of fine powder in their unprocessed state. After PGX processing though, pectin takes the form of interconnected fibrils giving the appearance of a highly interwoven structure (**Fig. 11**). Starch, on the other hand, comes out as very fine granules.

Prior to testing these materials for the production of AC, it is important to understand the thermal stability of these materials, as a result, the materials were first tested for thermal stability using thermogravimetric analysis (TGA). This was to determine if the PGX polymers offered any additional thermal stability post processing and identify the carbonization temperature where most of the volatile matter from the raw materials had been removed to give high carbon content final product. Once an adequate temperature range for carbonization was identified, the materials were used for the production of AC using two separate approaches namely:

1. **Direct Carbonization:** Under this approach, the raw materials (PGX or non PGX) were pyrolyzed without the use of any additional activating agents.
2. **Chemical Activation**: For this approach, prior to being pyrolyzed, the PGX polymers were treated with a chemical activating agent. Two different chemical agents namely zinc chloride and phosphoric acid, which are popular industrial activating agents as well were used for activation purpose.

There is a limited amount of literature data available on the possible use of these materials for the production of AC using the approaches described above. This would also be the first time that the PGX processed polymers will be tested for any kind of thermal treatment. The current study aims to establish the foundations of using polysaccharides for the production of AC and possibly determine causes for the variations (if any) in the results obtained between the PGX and non PGX polymers.

## 2.2 Materials

Corn starch (Sigma Aldrich S-4126) and zinc chloride (anhydrous, free-flowing, Redi-Dri™, ACS reagent, ≥97%) were bought from Sigma Aldrich, Canada. Pectin (TexDry LC Citrus) was obtained from Florida Food Products, Texas. PGX processed corn starch and pectin (of above mentioned brands) were provided by Ceapro Inc. Other reagents purchased were phosphoric acid 85 % (w/w) **(**Caledon Laboratory Chemicals**),** 0.1 N hydrochloric acid (LabChem) and 0.1 N sodium hydroxide (LabChem)

## 2.3 Methods

### 2.3.1 Thermogravimetric Analysis (TGA)

The production of AC requires the precursor to be pyrolyzed at high temperatures, so it is important to understand the thermal behaviour of the material first. TGA was used to determine the thermal stability of the raw materials and to decide upon a temperature range for the carbonization of the samples. The analysis was performed using *TA instruments Q50* analyzer under an argon atmosphere with ramp temperature of 10 $^{o}$C/min. The temperature range was 25 $^{o}$C – 600 $^{o}$C. Sample weight used was <10 mg for all samples and analysis was done in at least duplicate. The samples tested were corn starch and pectin and their respective PGX processed variants.

### 2.3.2 Direct carbonization

As the PGX materials are known to have high surface area and already have a developed pore network, it was hypothesized that carbonizing these materials could possibly produce porous carbon materials without having to use any other activation

or pore creation steps, the PGX structure would sustain the carbonization process and the final product would be porous carbon skeleton.

#### 2.3.2.1 Synthesis

Since the aim of this approach was to eliminate any pre processing steps prior to carbonization and let the PGX process solely dictate the pore formations, no pre treatments were done before the carbonization stage. 1-3 g of the polymer was added to a ceramic boat crucible, which was then placed inside a fused quartz tube which in turn was placed inside a horizontal single zone tube furnace (*Thermcraft Inc.*). The furnace temperature was then ramped at 5 $^{o}$C/min to the final carbonization temperatures (400-600 $^{o}$C) under a nitrogen atmosphere of flow rate 150 cc/min where it was maintained for another 2 hours.

The furnace was then allowed to cool (temp. <70 $^{o}$C) before the sample was taken out. The samples were then acid washed with 0.1 N HCl in order to remove any dissolvable residues and clear out any blocked pore, this was followed by multiple washes with de-ionized (DI) water. After washing, the samples were dried in an oven at 105 $^{o}$C for 24 hours and then transferred to a series of stainless steel mesh sieves stacked on top of each other. The mesh sizes used for screening were #30, #60, #80 and #120 and the contents were shaken by hand causing the particles to get separated based on their size. During sieving, it was observed that the highest mass of fraction retained was between #30 and #80, as a result, 30x80 fraction was used for all analysis purpose. Since this fraction corresponds to particle size < 1 mm, the AC being produced would be characterized as PAC.

Samples were also put aside where no post processing steps (washing or screening) were done in order to determine if the post processing steps had any significant impact on the SSA.

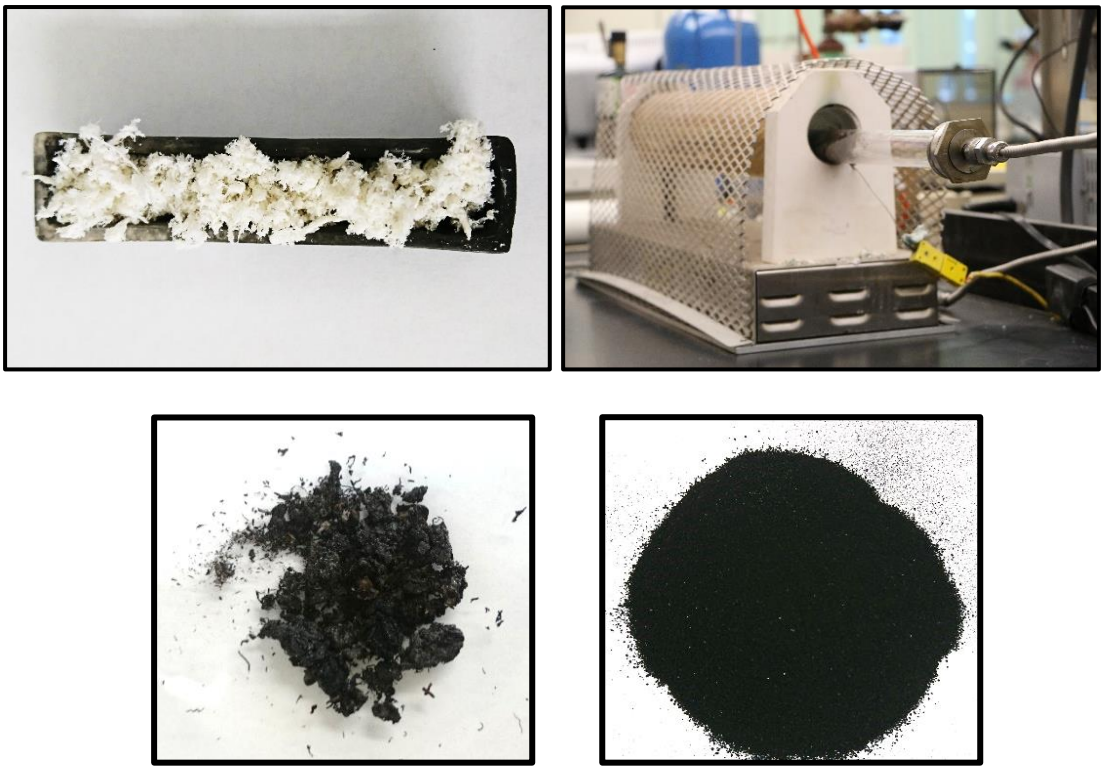

**Figure 12.** Photographs depicting the different stages of production of AC by direct carbonization method.

### 2.3.2.2 Characterization

The SSA along with the pore size and volume distribution of the samples were analyzed using nitrogen sorption at 77 K using the Quantachrome® ASiQwin surface area analyzer. Multi-point BET in the linear range (relative pressure 0-0.3) of the BET equation was used to determine the specific surface area. The samples were de-gassed under vacuum at 125 $^{o}$C for 24 hours prior to analysis. Due to the distorted graphitic structure of ACs, there are slit like voids between the sheets, as a result, the pore volume and pore size distribution were determined using the Quenched Solid Density Functional theory (QSDFT) [34] $N_2$ equilibrium model for slit pores.

The surface morphology of the raw material and the final ACs were imaged using SEM technique. Nickel paste was used as a conductive adhesive and the samples were imaged using the JEOL 6610LV SEM at accelerating voltage of 3kV and a working distance of 12-13 mm

### 2.3.3 Chemical activation

The second approach that was taken towards the creation of AC was the classical route through chemical activation. It was hypothesized that due to the porous structure of PGX materials the chemical agent might penetrate into the interiors of particles better, as compared to the unprocessed material giving rise to ACs with different pore structures. Popular industrial chemical agents, phosphoric acid and zinc chloride were selected as the activating agents.

#### 2.3.3.2 Preparation of activating agent

**Phosphoric acid:**

Since 85% (w/w) solution of acid was available as stock, dilution to lower concentrations was required. The dilutions were done using the below equation:

$$M_1V_1 = M_2V_2$$

Where $M_1$ and $M_2$ represent the initial and final molarities of phosphoric acid and $V_1$ and $V_2$ the volume required for each molarity. The conversion of concentration from w/w % to molarities was done using the below equation:

$$Molarity = \frac{10 \times Conc.\,\%\left(\frac{w}{w}\right) \times density\ solution}{molecular\ weight}$$

The densities of different concentrations of $H_3PO_4$ is provided in Table 4.

**Table 4** Densities of different concentrations of phosphoric acid solution

| **Concentration % (w/w)** | 85 (Stock) | 60 | 40 |
|---|---|---|---|
| **Density (g $cc^{-1}$)** | 1.68 | 1.42 | 1.25 |

**Zinc chloride:**

Since powdered zinc chloride was being used, solutions of zinc chloride were made by dissolving it in Milli-Q water. The density of the solutions was then measured by pipetting out 10 ml in a beaker and measuring the final mass. The densities of different solutions are provided below:

**Table 5** Densities of different concentrations of zinc chloride solution

| **Concentration % (w/w)** | 40 | 50 | 60 |
|---|---|---|---|
| **Density (g $cc^{-1}$)** | 1.4 | 1.53 | 1.69 |

**2.3.3.3 Preliminary testing**

In order to proceed further, the concept of impregnation ratio or mass ratio (MR) must be explained. Mass ratio refers to the ratio of the mass of the activating agent to the mass of raw material.

$$Mass\ ratio\ (MR) = \frac{mass\ of\ 100\%\ dry\ activating\ agent\ (g)}{mass\ of\ raw\ material\ (g)}$$

Since aqueous solutions of the activating agent are used, the volume of activating agent required is calculated by the following equation:

$$Volume\ (ml) = \frac{mass\ of\ raw\ material\ (g) \times multiplication\ factor \times mass\ ratio}{Density\ of\ activating\ agent\ solution\ (g\ cc^{-1})}$$

Where multiplication factor is related to the concentration of the activating agent.

$$Multiplication\ factor = \frac{100}{Concentration\ \%\ \left(\frac{w}{w}\right) of\ activating\ agent}$$

Since there was no prior information on the behavior of interaction of these materials with the selected activating agent, a preliminary trial was run to decide the concentration range of phosphoric acid to be used. 40 % (w/w) and 60 % (w/w) concentrations were used to carry out the trial run. 2 g of the raw material (starch or pectin) was added to a beaker and phosphoric acid solutions at mass ratio of 1 and 2 were added to the beakers and the contents were mixed together with a spatula. The contents were then left at room temperature for 15 hours to observe any change in behavior.

#### 2.3.3.4 Design of experiment with phosphoric acid as activating agent

In order to study if phosphoric acid could produce ACs with different pore structures using unprocessed and PGX processed variants of pectin, a design of experiment study was employed to investigate the effect of process parameters for the production of AC.

A $2^4$ full factorial design of experiment (DOE) study was designed to maximize the SSA (response) as well as to study the difference in the pore size distribution of the AC made from PGX and non PGX variant. The design parameters are listed in **Table 6.** The limits of DOE were based on previous studies that have using phosphoric acid as activating agent for the manufacturing of AC from agricultural residues [58] [39] [46].

**Table 6** Limits of DOE comparing PGX and non PGX AC from pectin using phosphoric acid as activating agent

| Factor | Low | High |
|---|---|---|
| Material | Non PGX | PGX |
| Temperature (°C) | 400 | 600 |
| Concentration % $H_3PO_4$ (w/w) | 40 | 85 |
| Mass Ratio | 1 | 2 |

#### 2.3.3.4.1 Synthesis

1 g of the raw material was added to a beaker, depending upon the mass ratio, the required volume of phosphoric acid was added using a syringe and the contents were mixed together with a spatula. The mixture was then left open to atmosphere for 15 hours. Next day, the mixture was transferred to a ceramic boat crucible which was then placed inside a fused quartz tube which in turn was placed inside a horizontal single zone tube furnace *(Thermcraft Inc.)*. The furnace temperature was then ramped at 5 °C/min to the final carbonization temperature under a nitrogen atmosphere of low rate 150 cc/min where it was maintained for another 2 hours. The furnace was then allowed to cool (<70 °C) before the sample was taken out. The samples were then base washed with 0.1 N NaOH in order to remove any dissolvable residues, clear out any blocked pore and neutralize the phosphoric acid, this was followed by multiple washed with DI water. After washing the samples were dried in an oven at 105 °C for 24 hours. The AC was then screened using mesh sieves following the same methodology outlined in section 2.3.2.1.

#### 2.3.3.4.2 Characterization

The AC made under different DOE conditions was characterized using gas sorption technique using the Quantachrome® ASiQwin surface area analyzer for the

determination of SSA and pore size distribution. The method of analysis remained the same as in section 2.3.2.2.

Scanning electron microscope (SEM) technique was employed to study the surface morphology of the AC. The samples were spread on carbon tape and coated with 5 nm of gold through sputter coating prior to imaging which was analysed using the VEGA TESCAN SEM at accelerating voltage of 10-30 eV and a working distance of 10-40 mm.

#### 2.3.3.5 Design of experiment with zinc chloride as activating agent

Zinc chloride, a common industrial activating agent was chosen as the second chemical to produce chemically AC. A similar approach as earlier was employed, but due to the shortage of raw material and to save time, a smaller DOE was designed this time. The mass ratio was fixed at 1.25.

A $2^3$ full factorial DOE study was designed to study the effect of the nature of the starting material, the concentration of activating agent and carbonization temperature on SSA (response). The limits of the DOE are listed in **Table 7**. The experimental data were fit with the help of Minitab software into a $2^{nd}$ degree regression model, and the Pareto plot, the normal effect plot and the p-value of the model terms were used to identify the significant factors affecting the response. AC for all DOE conditions was manufactured in duplicate to generate any results.

**Table 7** Limits for DOE comparing PGX and non PGX AC from pectin using zinc chloride as activating agent

| Factor | Low | High |
|---|---|---|
| Material | Non PGX | PGX |
| Temperature ($^oC$) | 400 | 600 |
| Concentration % $ZnCl_2$ (w/w) | 40 | 60 |

#### 2.3.3.5.1 Synthesis

The method of production remained the same as in section 2.3.2.1, with one minor change, the washing step involved washing with 0.1 N HCl instead of 0.1 N NaOH as earlier. This was done to dissolve any residual zinc chloride on the AC and to clear out any blocked pores.

#### 2.3.3.5.2 Characterization

The AC made under different DOE conditions were characterized using gas sorption technique using the Quantachrome® ASiQwin surface area analyzer for the determination of SSA and pore size distribution. The method of analysis remained the same as in section 2.3.2.2.

Scanning electron microscope (SEM) technique was employed to study the surface morphology of the AC. The samples were spread on double sided copper tape and coated with 3 nm platinum via sputter coating prior to analysis which was imaged using the FEI Magellan 400 SEM. Accelerating voltage was maintained at 1 kV and working distances used were 1-3 mm.

## 2.4 Results and Discussions

### 2.4.1 Thermogravimetric Analysis

Thermogravimetric analysis technique is used to understand the thermal stability of a polymer. As can be observed from **Fig. 13**, in the case of pectin (PGX or non PGX), the polymer is thermally stable until ~ 200 $^{o}$C, with an onset temperature of ~ 215 $^{o}$C. There onwards there is a continuous gradual mass loss till 400 $^{o}$C totaling ~50%. Beyond 400 $^{o}$C until 600 $^{o}$C the mass loss is < 15%. Similar behavior was obtained in case of the PGX processed pectin. The constituting molecules of pectin are D-galacturonic acid and depending on the source these acidic groups could be esterified to varying proportions. To understand if any variability in TGA exists, another source of pectin (pectin from citrus peel, galacturonic acid ≥74.0 %) was obtained from Sigma Aldrich and tested. No significant variation in the onset temperature (~215$^{o}$C) or the overall weight loss profile was observed, confirming that the source of pectin does not have any significant impact on the thermal behavior of the polymer.

For starch (both unprocessed and PGX processed) the on-set point is higher ~305 $^{o}$C compared to pectin, however, there is a sudden drop in mass ~50% in the range 300-325 $^{o}$C. Similar to pectin, there is minimal mass loss after 400 $^{o}$C.

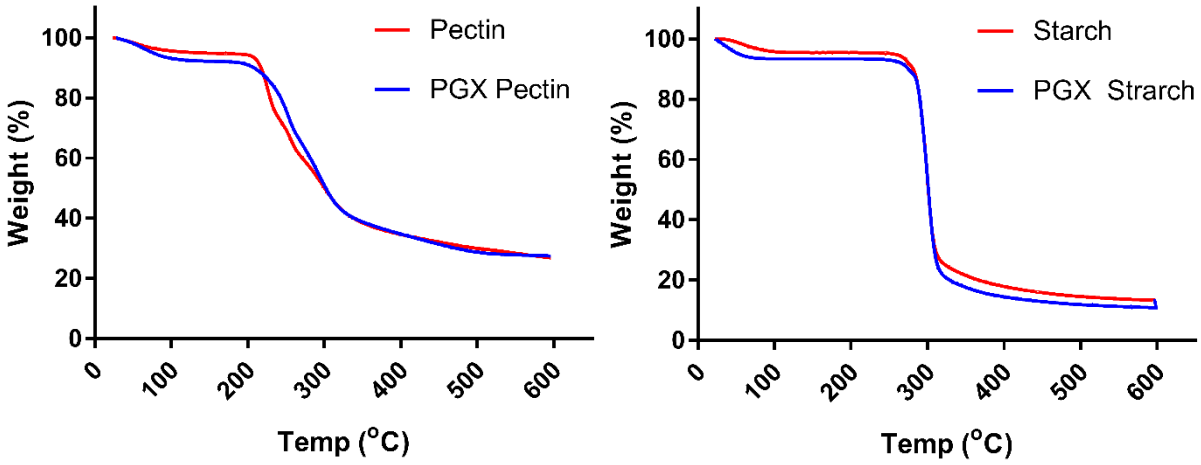


**Figure 13** TGA curves for pectin (left) and starch (right)

Comparing the unprocessed polymer to the PGX processed ones it was clear that the PGX polymers did not offer any additional thermal stability. This was also an indication that during the PGX process no new bond formations between the polymer molecules (such as cross linking between different branches of the polymer) takes place that might offer any additional structural strength thereby increasing the onset temperature and improving thermal stability.

In order to decide upon a temperature range for carbonization, it is important to work in a regime where the volatiles have exit the raw material leaving behind a carbon rich exoskeleton. From the TGA curves, it can be deduced that the carbonization temperatures have to be at least greater than 350 $^{o}$C. If carbonization was to be performed in the regime of 200-400 $^{o}$C, due to the rapidly changing chemical composition of the material (especially in the case of starch) it would be difficult to reproduce any results. Since one of the driving forces for this project was to be sustainable, it was decided to make the process conditions as less severe as possible. In order to achieve that goal, it is also important to be conservative in terms of energy consumption. Carbonization process requires the material to be pyrolyzed at high

temperature and higher the temperature, higher is the energy cost. To mitigate that it was decided to work in the temperature range of 400-600 $^{o}$C. Working at these temperatures also allows the presence of residual oxygenated surface groups on the AC since the material is not 100% carbonized. These surface groups as described earlier [24] also influence the adsorption behavior of the carbon.

### 2.4.2 Direct carbonization

#### 2.4.2.1 Specific surface area

The SSAs obtained along with total pore volumes under different conditions are listed in **Table 8.**

**Table 8** Results of gas sorption analysis (SSA and PV) using direct carbonization method.

| **Material** | **Temp. ($^{o}$C)** | **SSA ($m^2 g^{-1}$)** | **Total PV ($cc\ g^{-1}$)** |
|---|---|---|---|
| Starch | n/a | <5 | n/a |
| PGX Starch | n/a | 67 ± 8 | 0.296 ± 0.05 |
| Starch | 400$^{o}$C | <5 | n/a |
| Starch | 600$^{o}$C | <5 | n/a |
| PGX Starch | 400$^{o}$C | <5 | n/a |
| PGX Starch | 600$^{o}$C | <5 | n/a |
| Pectin | n/a | <5 | n/a |
| PGX Pectin | n/a | 320 ± 46 | 1.7 ± 0.38 |
| Pectin | 400$^{o}$C | <5 | n/a |
| Pectin | 600$^{o}$C | <5 | n/a |
| PGX Pectin | 400$^{o}$C | <5 | n/a |
| PGX Pectin | 600$^{o}$C | <5 | n/a |
| PGX Pectin** | 400$^{o}$C | <5 | n/a |
| PGX Pectin** | 600$^{o}$C | <5 | n/a |

** Refers to samples where no post processing steps (washing or sieving) were employed.

The unprocessed starch or pectin as expected did not offer any significant SSA or porosity in their native state. However evident from the gas sorption data, the PGX processed polymers had noticeably higher SSA than the unprocessed counterparts,

especially in the case of pectin. Looking at the gas sorption isotherm for PGX pectin (**Fig. 14**), it is clear that the isotherm shape resembles type III indicating a primarily mesoporous material. The sharp increase in adsorption at relative pressures approaching unity is due to rapid multilayer adsorption of nitrogen molecules on top of each other. The chosen pore size distribution model (QSDFT) evaluates the pore size in the range of 0-40 nm and the pore volume distribution from this model provides an insight into the mesoporous nature of the materials as the entire pore volume (~100%) was contributed by the mesopores. However as there is a sharp increase in the cumulative pore volume (**Fig. 14**), and it does not flatten out before 50 nm, it is an indication that there are pores beyond 50 nm in size which would add to the macroporous characteristics of the material.

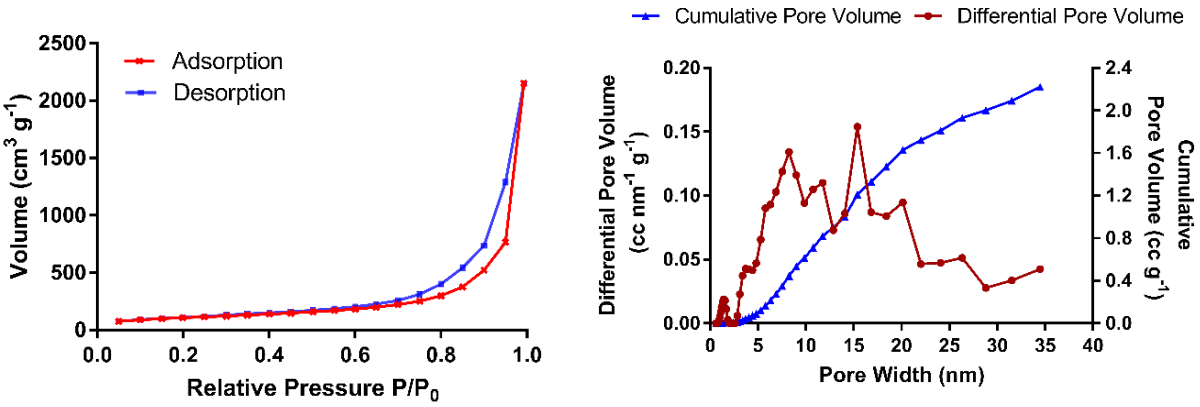


**Figure 14**. Gas sorption isotherm (left) and pore size distribution (right) for PGX processed pectin.

It should be clarified here that while there is a significant large variation between the SSA of starch and pectin, it is not due to any operational factors. Every polymer responds differently inside the PGX vessel, hence giving rise to different morphologies and pore structures. It has been observed that after PGX processing starch comes out as fine or coarse granules while pectin takes the shape of

interconnected layered sheets. This variation in behavior inside the vessel causes the SSA to be so different among different materials.

However, post carbonization there was no significant increase in the SSA for any of the raw materials (PGX or non PGX), in fact, the PGX processed polymers had lost all of their initial surface area as well. This can be attributed to the fact that there was no activating agent to create new pores or prevent the collapse of existing pores. The material was simply being pyrolyzed with no controlling agent. Both large and small molecules volatilized, leaving behind molecular size pores and in the course of time, these pores collapsed. The isotherms generated through gas sorption carried no significance since there was neither any surface area nor pore volume offered by these materials essentially just producing char.

It was concluded that the PGX structure was not strong enough to sustain the pyrolysis conditions and there was no measurable way to distinguish between the PGX and non PGX materials post carbonization. Any advantage that the PGX materials offered before in terms of surface area were completely lost post carbonization. This can also be traced back to the TGA results that revealed that the PGX polymers did not offer any additional thermal stability. The meso/macro porous nature of the polymers made it susceptible to collapse as the pores could resist the severe conditions of carbonization.

This is in contrast to the Starbon™ process, where the gelation step leads to the formation of strong covalent bonds which are able to sustain the drying and carbonization steps later maintaining the mesoporous structure [57]. The pores formed during the PGX process are not due to any permanent bonds, but simply individual

particle bound loosely to one another. As a result, they are susceptible to collapsing under severe conditions.

It should also be pointed out here that significant tar formation was observed in the case of carbonization of pectin, where there was visible yellow residue on the walls of the quartz tube. It is known that using an activating agent limits the formation of tar [25] which was not the case in for this approach where there was no activating agent used.

There was another noticeable phenomenon that was observed was that in case of carbonization of starch. There seemed to be an expansion of starch particles that occurred during carbonization as an expanded charred starch was obtained after the process (**Fig. 15**). This expansion behavior was observed in every instance when starch was carbonized.

**Figure 15.** The observed foaming of starch during carbonization

Similar phenomena have been reported in the past, where during the carbonization process, starch goes through numerous physio-chemical changes, one of which is the "molten starch" phase [59], which occurs immediately after the meting of individual starch particles at around ~250 $^{o}$C . This is followed by the expansion of the liquid matrix to form a foam like structure and further heating causes the degradation of the

starch molecules leading to the formation of numerous aromatic compounds, most significant of which is levoglucosan [60]. Since it was not possible to monitor the changes inside the furnace, only the final form of the expanded starch that had already cooled down and taken solid shape could be noticed. This, however, offered no contribution to the SSA obtained as the values remained almost negligible in all cases.

#### 2.4.2.2 Surface morphology of raw material and activated carbon

Due to the non conductive nature of the polymers, it was difficult to get sharp and clear images of the raw materials through SEM. Pectin could still be viewed at moderately high resolutions but there would occur excess charging and drift phenomena for the starch samples. Working distances < 10 mm lead to significant charging issues making it impossible to capture high resolution images. The images at the obtained resolution would only reflect that the PGX polymer was in form of layered sheets and fibrils. For the carbonized polymer visible charring could be noticed with more layers detectable at higher resolutions. However, no defined pore structure could be detected for any of the samples.

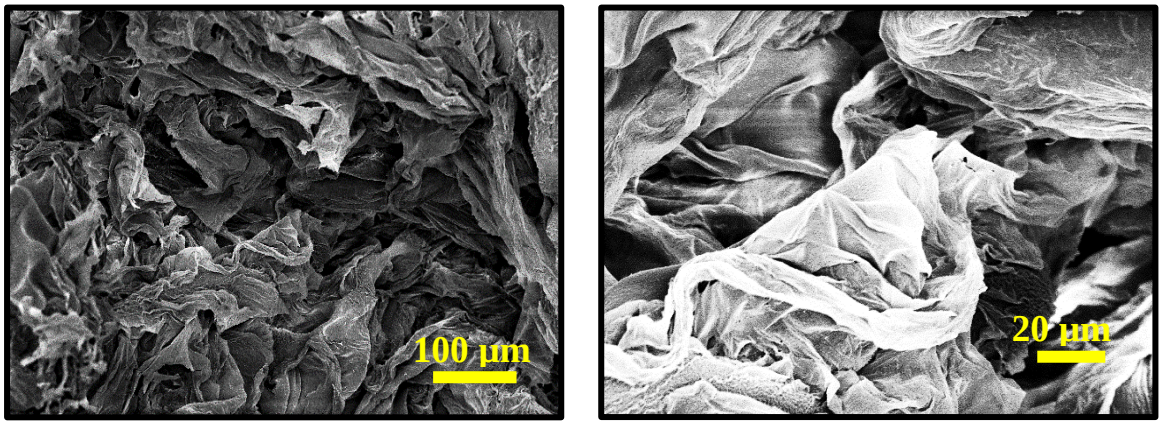


**Figure 16.** SEM images of PGX processed pectin. The layered structure of the PGX polymer could be visualized, however, at higher resolutions (right), noticeable charging was observed and it was difficult to capture good images.

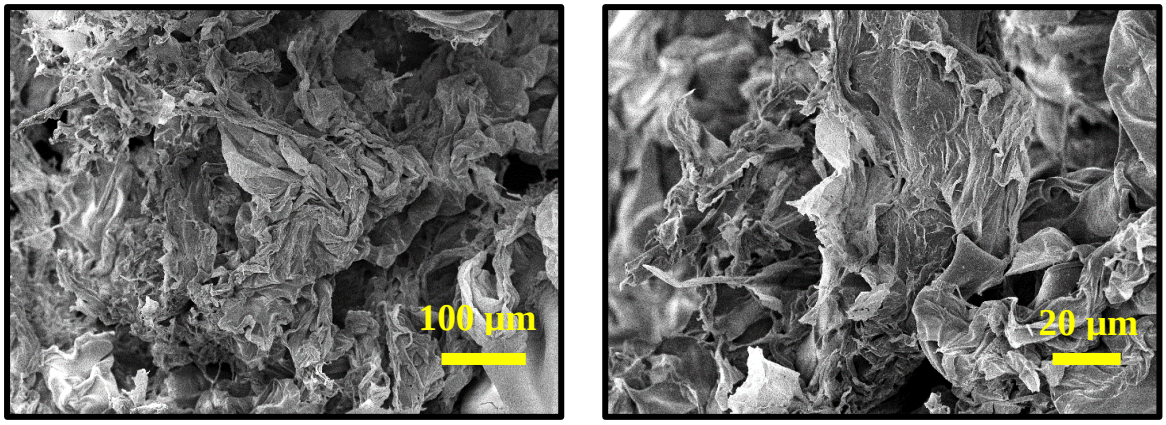


**Figure 17**. SEM images of PGX pectin carbonized at 400 °C. Noticeable charring of the individual layers could be observed however no conclusive argument regarding the pore structure could be made at such resolutions.

### 2.4.3 Chemical activation

#### 2.4.3.1 Preliminary test

The preliminary test was run to identify the behaviour of the interaction between the chemical agent and the polymer in order to decide upon the concentration range of the activating agents. Based on initial test it was observed that starch (PGX or non PGX) formed a liquid suspension when mixed with 40% phosphoric acid (MR 1 or 2) making it impractical to carbonize the material. At 60% concentration, it would form a gelatinous mass which could be carbonized. However, it was observed that soon enough the activating agent would completely hydrolyse the starch leaving behind a wet tarry residue, once again making it impractical to carbonize the material.

Since the PGX structure would have already been destroyed during the hydrolysis, there was no reason to continue the study further with starch. It was also concluded that for all for all concentration less than 40%, the suspension behavior would be observed, and for concentrations greater than 60%, the formation of gelatinous mass followed by hydrolysis into tar will be observed.

In the case of pectin, at both 40% and 60% phosphoric acid concentrations, pectin (all forms) would not form a liquid suspension although the 40% mixture was relatively wet. At 60% concentration, it would not undergo any significant hydrolysis or decompose to form any tar. Noticeable hydrolysis was observed for both concentration case by the change in colour of pectin from light brown to a slightly darker shade.


**Figure 18.** The behavior of PGX starch on the addition of phosphoric acid. From 1&2 it was observed that when starch was mixed with 40% phosphoric acid at a MR of 1 or 2, it formed a liquid suspension with the PGX structure being completely destroyed. At 60% concentration (3&4), it formed a gelatinous mass (5). However overtime phosphoric acid completely hydrolysed the mass leaving behind a wet tarry residue (6) the next day.

Although, upon the addition of phosphoric acid, a visible collapse of the PGX structure was observed, even so, the collapsed structure still resembled the initial PGX polymer in some capacity. Also, it should be pointed out here that due to the highly

expanded nature of the PGX polymer, it was difficult to uniformly mix the activating agent with the polymer and there were visible areas where no contact with the activating agent had taken place.

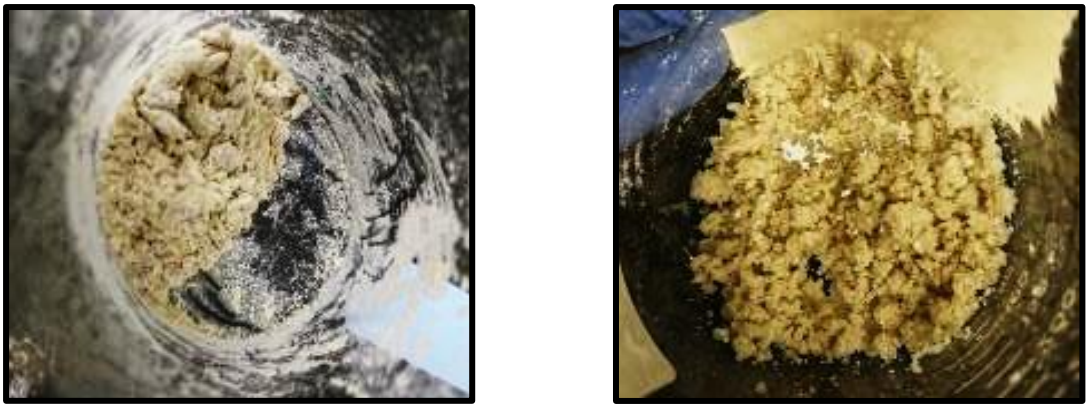

**Figure 19**. The behavior of pectin when mixed with 40% phosphoric acid (MR 1). Unprocessed pectin (left) formed small dry agglomerates, and its PGX counterpart (right) formed similar agglomerates with the noticeable collapse of the PGX structure.

Through the preliminary test, it was concluded that starch was unsuitable for chemical activation process using phosphoric acid. Also given the issues (expansion of starch) that were noticed during direct carbonization as well as the minimal increase in the surface area offered by PGX processed starch, it was decided not to continue any further studies with starch.

### 2.4.3.2 Phosphoric acid as activating agent

#### 2.4.3.2.1 Specific surface area and pore size distribution

During the BET analysis of phosphoric acid AC from pectin, numerous issues were faced especially with respect to reproducibility of results and more so in obtaining credible isotherms. The results of the study are listed in **Table 9.**

**Table 9** Results of gas sorption analysis (SSA and PV) comparing PGX and non PGX pectin AC using phosphoric acid as activating agent.

| Sl. | Material | Temp. (°C) | $H_3PO_4$ Conc. % (w/w) | MR | SSA ($m^2$ $g^{-1}$) | Total PV (g $cc^{-1}$) |
|---|---|---|---|---|---|---|
| 1 | Non PGX | 400 | 40 | 1 | 619 ± 438 | 0.45 ± 0.33 |
| 2 | PGX | 400 | 40 | 1 | 310 ± 221 | 0.21 ± 0.17 |
| 3 | Non PGX | 600 | 40 | 1 | 374 | 0.326 |
| 4 | PGX | 600 | 40 | 1 | 384±377 | 0.25 ± 0.23 |
| 5 | Non PGX | 400 | 85 | 1 | 244 | 0.2 |
| 6 | PGX | 400 | 85 | 1 | 255 | 0.26 |
| 7 | Non PGX | 600 | 85 | 1 | <5 | n/a |
| 8 | PGX | 600 | 85 | 1 | 259 | 0.21 |
| 9 | Non PGX | 400 | 40 | 2 | <5 | n/a |
| 10 | PGX | 400 | 40 | 2 | 165 ±176 | 0.03 ± 0.005 |
| 11 | Non PGX | 600 | 40 | 2 | <5 | n/a |
| 12 | PGX | 600 | 40 | 2 | 37 | 0.1 |
| 13 | Non PGX | 400 | 85 | 2 | <5 | 0.002 |
| 14 | PGX | 400 | 85 | 2 | 729 | 0.4 |
| 15 | Non PGX | 600 | 85 | 2 | <5 | n/a |
| 16 | PGX | 600 | 85 | 2 | 150 ± 149 | 0.16 ± 0.14 |

**Table 9** revealed that while there was a considerable increase in SSA compared to the results obtained through direct carbonization route earlier, it was also evident that massive variations with up to 90% coefficient of variation existed between different batches of the material made under identical conditions. Multiple trials were done both at McMaster University and the University of Waterloo (*instrument-Quantachrome® ASiQwin*) for determination of SSA and lead to highly variable results. Values as high as 1000 $m^2$ $g^{-1}$ were obtained under some conditions, but the values dropped to < 10 $m^2$ $g^{-1}$ at other conditions which did not make scientific sense.

Since each BET run took at least 48 hours (de-gassing + analysis time), a large portion of the time was being consumed for the analysis. Multiple de-gassing conditions (drying time and degassing temperatures) were also tested for some conditions to understand if any of those factors were having any impact but unfortunately no conclusive argument could be made.

Since the measurements were being done at random (from the DOE design) it made it extremely tough to proceed to other conditions without getting credible results first. Apart from the BET values themselves, the isotherms generated were highly irregular and lacked the credibility to predict any sort of pore structure from them. A set of erroneous isotherms obtained are presented in **Fig. 20.**

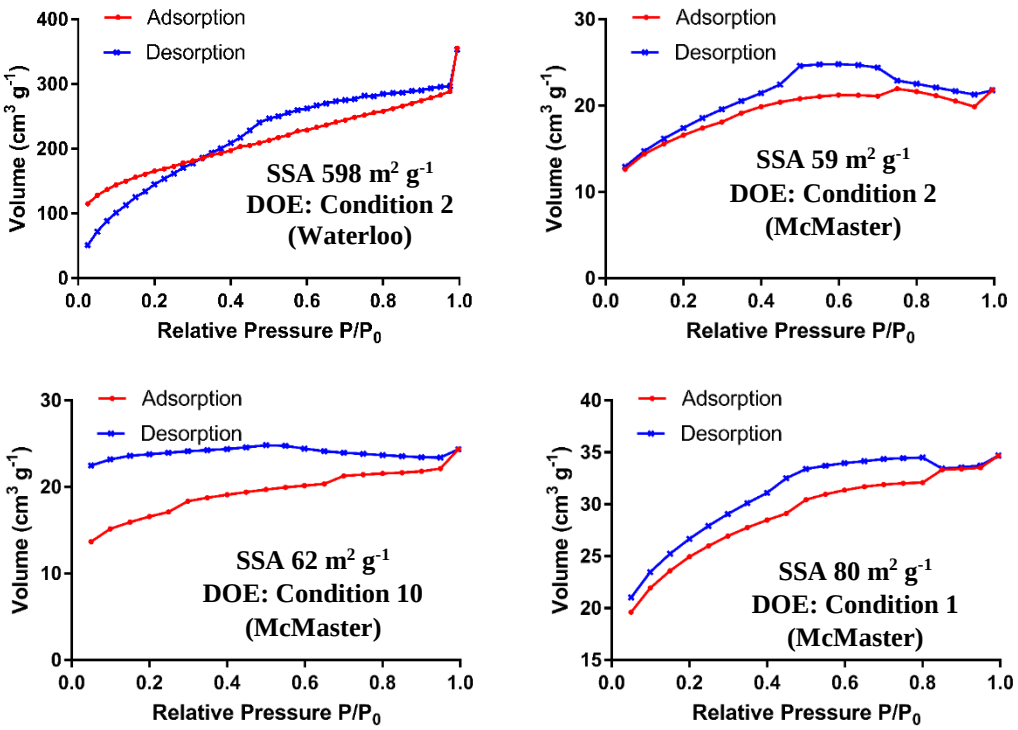


**Figure 20**. Example of erroneous isotherms. Surface area values calculated from these isotherms are not credible.

#### 2.4.3.1.2 Surface morphology of activated carbon

SEM technique was used to study the surface morphology of the AC, the results for which are presented in **Fig. 21.**

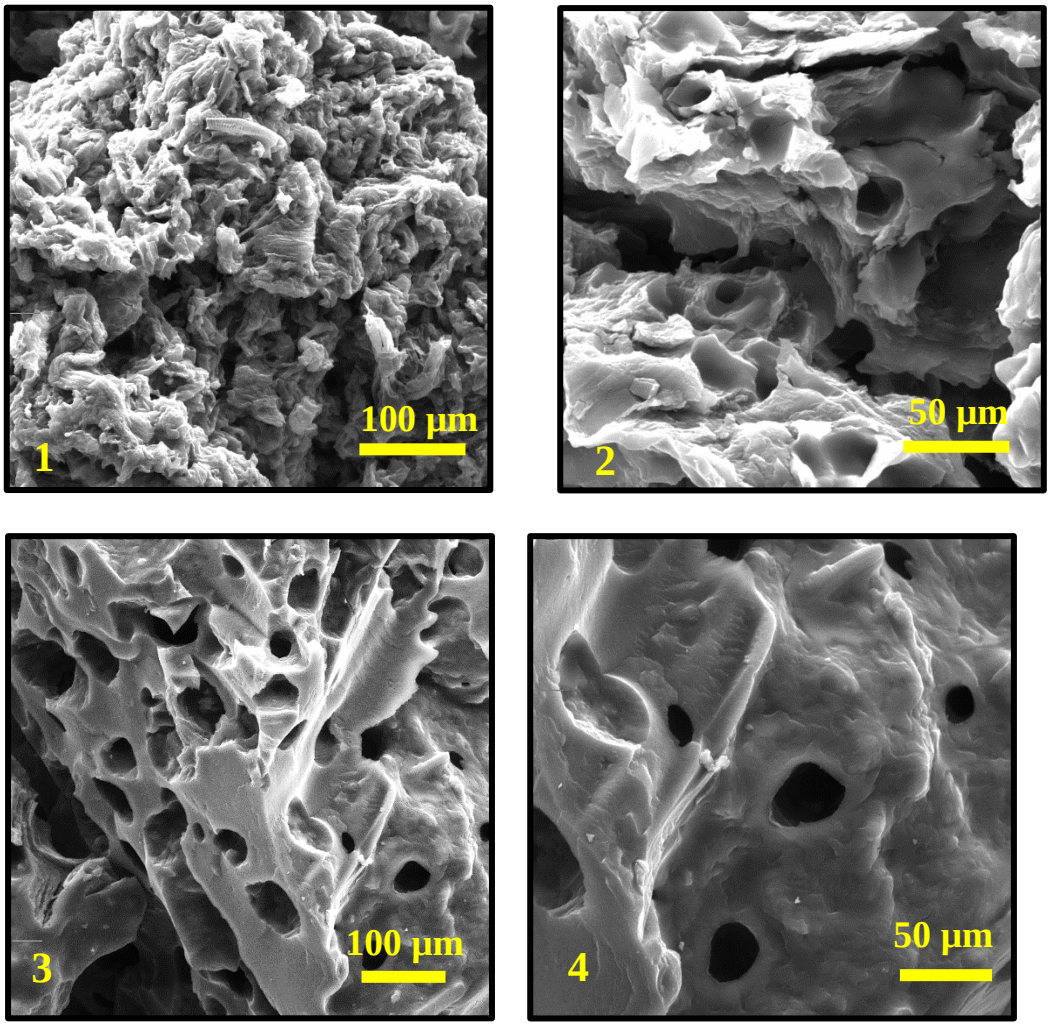


**Figure 21**. SEM images (1&2) of AC from PGX pectin (DOE Condition 2), a highly layered structure was visible and the SSA for this sample was more 500 $m^2 g^{-1}$. Images (3&4) revealed the surface morphology of AC from PGX pectin (DOE conditions 10), a relatively smooth structure with micrometer sized pores was prominent under this condition which had a SSA of 62 $m^2$ $g^{-1}$. The two conditions differed solely by the MR of phosphoric acid, making it improbable to predict any generalized trend regarding the surface morphology.

Several hypotheses could be proposed for the observed irregularities in the result obtained. Phosphoric acid is a severe chemical agent and, given the soft nature of the

starting polymer, it is possible that the acid was causing severe hydrolysis reactions and degrading the polymer chains. It had already been observed in the case of starch which was getting completely decomposed to tar. An appropriate analogy would be the reaction between sulphuric acid and sugar, where the acid completely decomposes the sugar molecules.

While during carbonization, there was definitely the development of a pore structure as indicated by the gas sorption data under certain conditions, however, it is proposed that the pores formed were not mechanically strong and collapsed during the course of carbonization and during the post processing stages. It is also possible that the mass ratios selected were higher than they should have been and better results could have been obtained at lower mass ratios. Essentially the final product being obtained was just char having no significant surface area or porosity.

The irregularities in the isotherms obtained also indicate the fragility of the pores. It is known that condensation of the gas molecules takes place in the mesopores during the adsorption step [30]. The liquid formed exerts pressure on the walls of the pores, and if the pores are not mechanically strong, they are susceptible to collapse during the desorption step, when the liquid starts evaporating.

Taking into consideration the large amount of time that was being invested in the manufacturing of AC under each condition (24 hours each) and BET analysis (at least 48 hours) combined with the results which at best were average compared to SSA of commercial ACs, it was decided that it would be best not to do any detailed investigation in these set of experiments.

It was during the same time that significant success while working with zinc chloride as an activating agent was achieved. Given the limited availability of the PGX processed polymers, it was decided to stop using phosphoric acid as an activating agent and instead move to zinc chloride.

#### 2.4.3.3 Zinc chloride as activating agent

##### 2.4.3.3.1 Statistical analysis of design of experiment

The DOE was designed for maximization of the SSA. The result of gas sorption analysis is presented in **Table 10**.

**Table 10** Results of gas sorption analysis (SSA and PV) comparing PGX and non PGX AC from pectin using zinc chloride as activating agent.

| Sl. | Material | Temp. ($^o$ C) | $ZnCl_2$ conc. % (w/w) | SSA ($m^2\ g^{-1}$) | Total PV ($cc\ g^{-1}$) |
|---|---|---|---|---|---|
| 1 | Non PGX | 400 | 40 | 2492 ± 28 | 1.28 ± 0 |
| 2 | PGX | 400 | 40 | 2088 ± 96 | 1.07 ± 0.035 |
| 3 | Non PGX | 600 | 40 | 2217 ± 233 | 1.11 ± 0.094 |
| 4 | PGX | 600 | 40 | 1943 ± 168 | 0.97 ± 0.085 |
| 5 | Non PGX | 400 | 60 | 1913 ± 12 | 0.96 ± 0.025 |
| 6 | PGX | 400 | 60 | 1729 ± 112 | 0.91 ± 0.060 |
| 7 | Non PGX | 600 | 60 | 2084 ± 110 | 1.02 ± 0.040 |
| 8 | PGX | 600 | 60 | 1818 ± 44 | 1 ± 0.015 |
| 9 | Non PGX | 500 | 50 | 2414 ± 59 | 1.22 ± 0.020 |
| 10 | PGX | 500 | 50 | 1917 ± 154 | 1.11 ± 0.085 |

The results of the SSA obtained were significantly higher than any of the previous methods used. SSAs exceeding 2000 $m^2\ g^{-1}$ and total pore volume > 1 $g\ cc^{-1}$ were obtained almost under all conditions. However, there appeared to be no significant

difference when comparing the PGX polymer to the unprocessed one. In fact, under all conditions, the PGX polymers seemed to have slightly lower SSAs. This can be attributed to two reasons. The first deduction is based on the TGA analysis that the PGX structure did not offer any additional thermal stability compared to the unprocessed polymer, as a result, once the polymer was fed to the furnace, the remaining structure collapsed and behaved exactly the same way as the unprocessed polymer. The second reason for the slightly low surface areas can be explained from experimental observations. Due to the expanded nature of the polymer, it was difficult to uniformly mix the activating agent with the polymer and there were visible regions where the activating agent had not come in contact with the polymer.

From the ANOVA analysis (**Table 11**) the Pareto plot (**Fig. 22**) and the normal effect plot (**Fig. 22**), it was observed that the material type followed by the concentration of zinc chloride had the most significant impact on the SSA (p value < 0.05). Unfortunately, it was the non PGX polymer that gave the better results. Since there is no difference in the chemical structure between PGX and non PGX pectin and material type is a categorical variable, material type is not a statistically significant factor that should be considered here. From the effect table (**Table 12**), it can be seen that no individual parameter had a positive impact when going from its low to high setting. Only the interaction between temperature and concentration had a reasonable positive impact when both were at high values (net effect of 152). It is quite possible that due to a limited range of the concentrations of activating agent and carbonization temperatures that were tested, the response obtained under different conditions are only marginally different from one another. It may be possible to get a more variable response by increasing the range of limits of the DOE variables.

**Table 11** ANOVA table for DOE comparing PGX and non PGX AC from pectin using zinc chloride as activating agent.

| Source | DF | Adj SS | Adj MS | F-Value | P-Value |
|---|---|---|---|---|---|
| Model | 7 | 1129198 | 161314 | 7.53 | 0.001 |
| Linear | 3 | 943816 | 314605 | 14.69 | 0.000 |
| **Material** | **1** | **540218** | **540218** | **25.23** | **0.000** |
| Temperature | 1 | 1958 | 1958 | 0.09 | 0.768 |
| **Concentration** | **1** | **401639** | **401639** | **18.76** | **0.001** |
| 2-Way Interactions | 3 | 114994 | 38331 | 1.79 | 0.203 |
| Material*Temperature | 1 | 150 | 150 | 0.01 | 0.935 |
| Material*Concentration | 1 | 22276 | 22276 | 1.04 | 0.328 |
| **Temperature*Concentration** | **1** | **92568** | **92568** | **4.32** | **0.060** |
| Curvature | 1 | 70389 | 70389 | 3.29 | 0.095 |
| Error | 12 | 256948 | 21412 | | |
| Total | 19 | 1386147 | | | |

**Table 12** Effect table for DOE comparing PGX and non PGX AC from pectin using Zinc chloride as activating agent.

| Term | Effect | Coef | SE Coef | T-Value | P-Value | VIF |
|---|---|---|---|---|---|---|
| Constant | | 2044.2 | 36.6 | 55.88 | 0.000 | |
| Material | -328.7 | -164.4 | 32.7 | -5.02 | 0.000 | 1.00 |
| Temperature | -22.1 | -11.1 | 36.6 | -0.30 | 0.768 | 1.00 |
| Concentration | -316.9 | -158.4 | 36.6 | -4.33 | 0.001 | 1.00 |
| Material*Temperature | -6.1 | -3.1 | 36.6 | -0.08 | 0.935 | 1.00 |
| Material*Concentration | 74.6 | 37.3 | 36.6 | 1.02 | 0.328 | 1.00 |
| **Temperature*Concentration** | **152.1** | **76.1** | **36.6** | **2.08** | **0.060** | **1.00** |
| Ct Pt | | 148.3 | 81.8 | 1.81 | 0.095 | 1.00 |

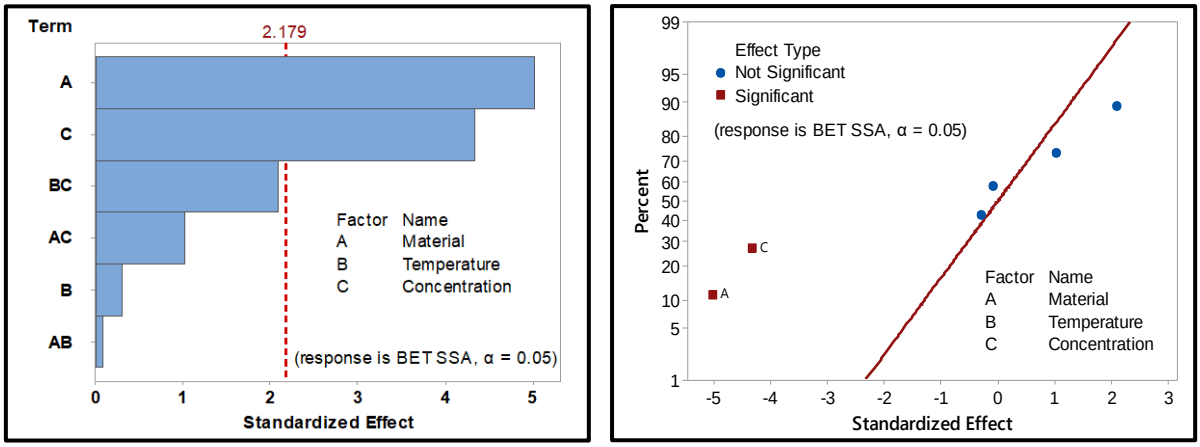


**Figure 22**. Pareto plot (left) and standard effect plot (right) for DOE comparing PGX and non PGX AC from pectin using zinc chloride as the activating agent.

### 2.4.3.3.2 Pore size and pore volume distribution

The isotherms obtained from $N_2$ sorption are presented in **Fig. 23.** It was apparent that all the isotherms represented Type I with an H4 hysteresis loop indicating that the AC was primarily microporous but there were mesoporous regions that were causing the capillary condensation as observed by the hysteresis loop. This observation was further confirmed by the pore size distribution for all the DOE conditions **Fig. 24**, where more than 70% of the total pore volume was contributed by the micropores even exceeding 80% under certain conditions. Even for the mesoporous volume, less than 5% of the total pore volume was contributed by pores greater than 5 nm in size making the ACs predominantly microporous. The distribution of pore volume is tabulated in **Table 13**.

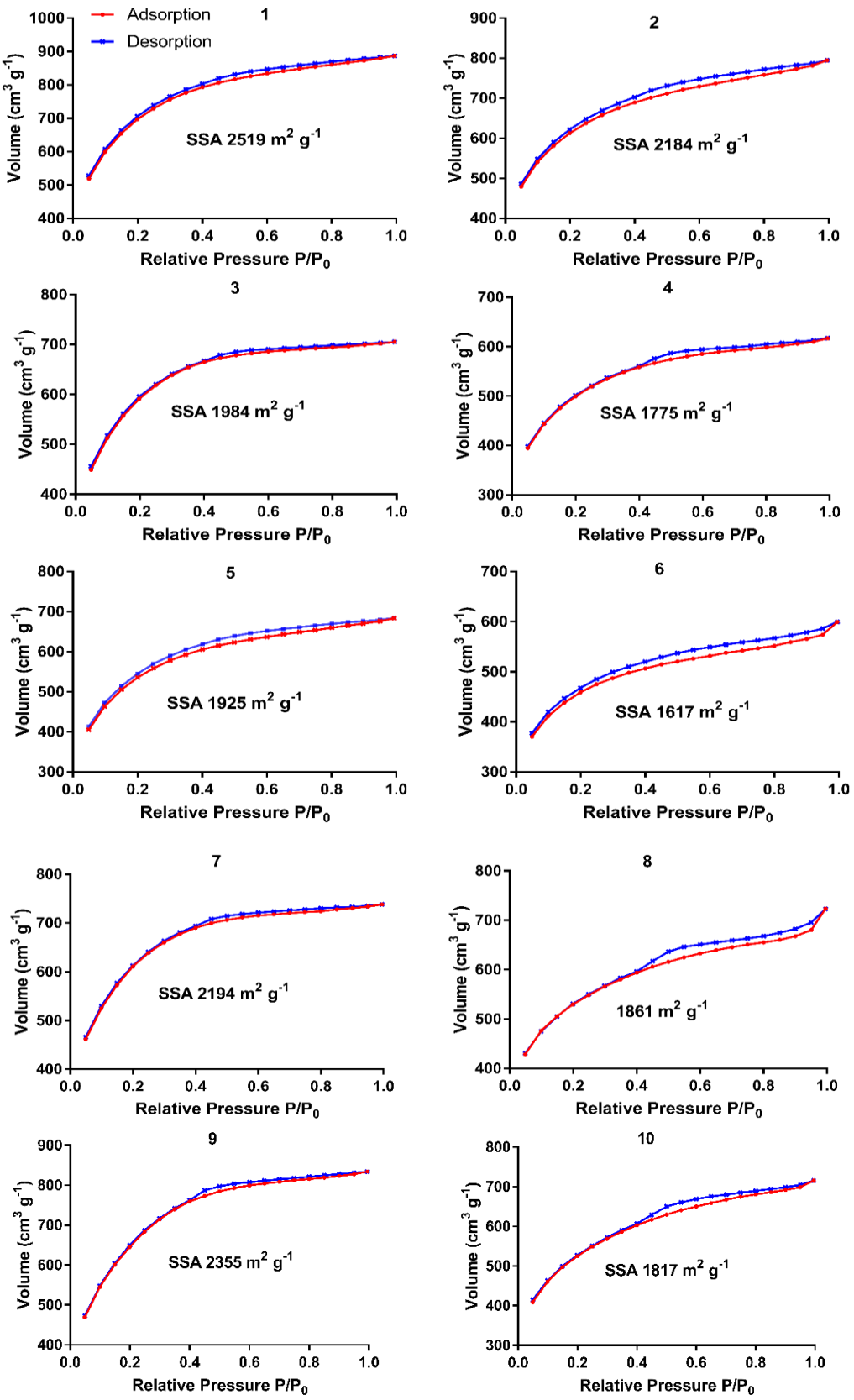


**Figure 23.** Gas sorption isotherms for ACs from DOE comparing PGX and non PGX AC from pectin using zinc chloride as activating agent. Serial numbers (1-10) indicate the DOE conditions corresponding to Table 10.

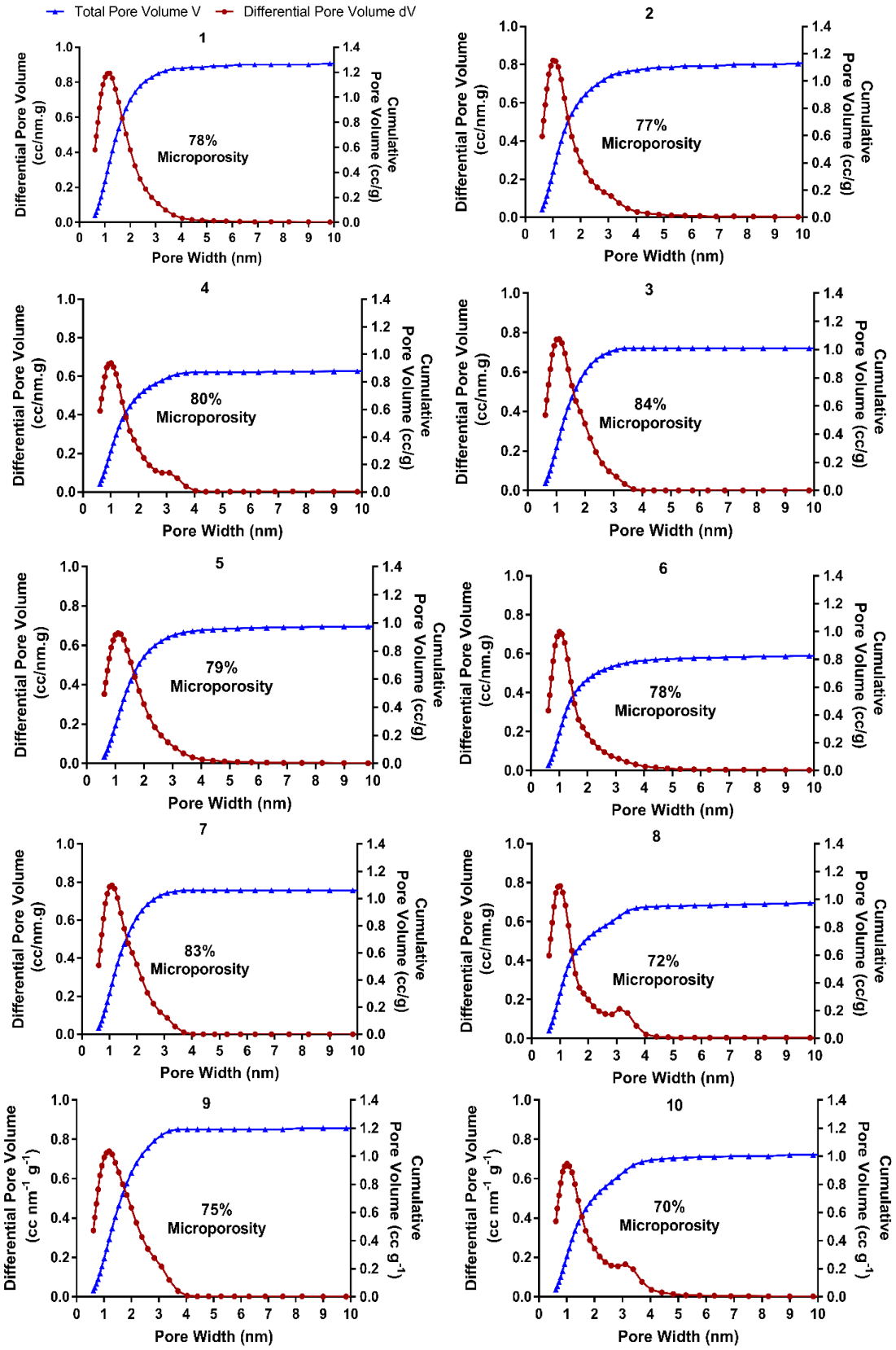


**Figure 24**. Pore size distribution of ACs from DOE comparing PGX and non PGX AC from pectin using zinc chloride as activating agent. Serial numbers (1-10) indicate the DOE conditions corresponding to Table 10.

**Table 13** Pore volume distribution of ACs comparing PGX vs non PGX AC from pectin using zinc chloride as activating agent.

| Sl. | Material | Temp. (ºC) | Conc. % (w/w) | % Total PV (< 2 nm) | % Total PV (2-5 nm) | % Total PV (> 5 nm) |
|---|---|---|---|---|---|---|
| 1 | Non PGX | 400 | 40 | 78 | 20 | 2 |
| 2 | PGX | 400 | 40 | 77 | 20 | 3 |
| 3 | Non PGX | 600 | 40 | 84 | 15 | <1 |
| 4 | PGX | 600 | 40 | 80 | 18 | 2 |
| 5 | Non PGX | 400 | 60 | 78 | 20 | 3 |
| 6 | PGX | 400 | 60 | 78 | 16 | 6 |
| 7 | Non PGX | 600 | 60 | 82 | 17 | <1 |
| 8 | PGX | 600 | 60 | 72 | 22 | 6 |
| 9 | Non PGX | 500 | 50 | 75 | 24 | 1 |
| 10 | PGX | 500 | 50 | 70 | 26 | 4 |

#### 2.4.3.3.3 Surface morphology of activated carbon

The SEM images obtained are presented in **Fig. 25**. In either case (PGX or Non PGX), a massive network of a porous web like structure was noticeable. These pores are distributed throughout the surface of the AC and it was evident that these nano-sized pores are responsible for contributing to the high values of SSA values obtained earlier.

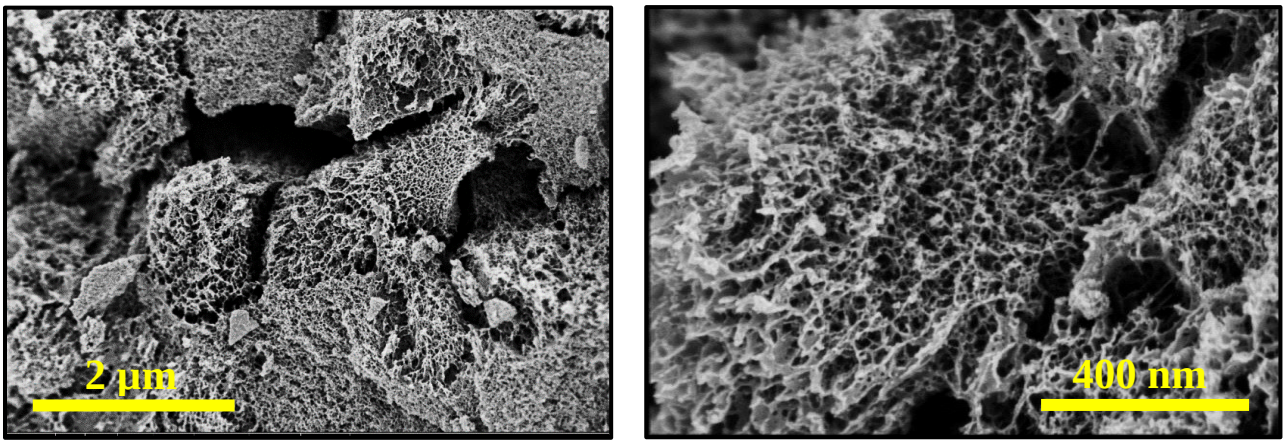


**Figure 25**. SEM images for AC from PGX pectin (DOE: Condition 8). A massive network of nano-sized pores was visible that was contributing to the exceptionally high surface areas obtained. Similar images were obtained for other conditions for both PGX processed and unprocessed pectin

## 2.5 Conclusions

The primary aim of this study was to compare the PGX processed polymers to unprocessed ones for the production of AC. Through this work, it has been observed that possibly due to the fragile nature of the PGX polymers, the PGX structure is almost entirely lost during carbonization making it lose all its initial pore structure and extended surface area.

When exposed to an activating agent ($H_3PO_4$ or $ZnCl_2$), an immediate collapse of the PGX structure was noticed (for pectin), and post carbonization it was difficult to differentiate between the unprocessed and PGX processed polymers. Starch was found to be unsuitable to be used as a raw material through chemical activation technique (when treated with $H_3PO_4$), undergoing rapid hydrolysis and decomposing to form tar.

The interaction between $H_3PO_4$ and pectin was a unique one as highly variable results under the same condition were obtained. High SSAs were obtained under certain conditions but it would seem that the mass ratios used were too high which might have lead to excessive hydrolysis of the parent polymer network leading to variable

and difficult to reproduce results.The interaction between pectin and $ZnCl_2$ was found to be highly favorable for the production of high SSA microporous AC. Although no significant differences were obtained between the PGX vs unprocessed pectin samples, the SSAs obtained for either of them exceeded 1800 $m^2/g$ even at a relatively mild temperature of 400 $^oC$ making it an interesting set of results that required further investigation.

The present work explored the use of activating agent by making working solutions based on calculations of mass ratio and initial concentration of the activating agent. This lead to variable volumes of the activating agent for the same mass ratio for different concentrations. These variable volumes lead to non-uniform mixing of the activating agent on the surface of the raw material particularly in the case of PGX processed pectin which had far more surface to be covered. To negate this effect, and to best utilise the surface of the PGX polymer, a fixed volume of the activating agent that would be sufficient to cover the entire surface of the polymer could be used.

# CHAPTER 3: Manufacturing of microporous carbon from pectin: Process optimization and characterization

## 3.1 Introduction

In the previous chapter, a study was conducted to investigate the possibility of using two different polysaccharides namely starch and pectin for the production of AC using PGX and non PGX processed variants. The results of the study revealed that starch was unsuitable for the production of AC using chemical activation and that the PGX processed polymers did not offer any significant advantage over the unprocessed polymers in terms of the SSA values obtained when used for the production of AC. However, some interesting results while using pectin as the raw material and zinc chloride as the activating agent were obtained, which resulted in the creation of high surface area AC with SSA exceeding 2000 $m^2$ $g^{-1}$ and the AC was revealed to have a high degree of microporosity (~80%). This chapter focuses on optimizing the process parameters for maximization of the SSA, tuning the porosity as well as analyzing the physicochemical characteritics of the AC. The AC will also be tested to determine its adsorption capacity for the removal of heavy metals ions (lead and cadmium) from water. Since the PGX processed pectin did not offer any notable advantage, this study will focus solely on unprocessed (non PGX) pectin.

## 3.2. Materials and Methods

### 3.2.1 Materials

Pectin (TexDry LC Citrus) was obtained from Florida Food Products, Texas. Zinc chloride (anhydrous, free-flowing, Redi-Dri™, reagent grade, ≥ 98%), lead (II) nitrate (≥99.95% trace metals basis), cadmium nitrate tetrahydrate were bought from Sigma Aldrich, Canada. Standard ICP solutions for lead (TraceCERT®, 1000 mg/L Pb in nitric acid) and cadmium (TraceCERT®, 1000 mg/L Pb in nitric acid) were also purchased from Sigma Aldrich. Commercial AC Hydrodarco 3000 was obtained from Cabot Norit, California.

### 3.2.2 Design of experiment for maximization of specific surface area

Since during the previous study with zinc chloride, the mass ratio was kept constant at a value of 1.25, it was necessary to study the effect of mass ratio to fully understand the behavior of the interaction between pectin and zinc chloride. A $2^3$ full factorial study was designed to study the effect of carbonization temperature, the concentration of activating agent (zinc chloride) and the mass ratio (MR) of the activating agent on SSA (response). The limits of the DOE are listed in **Table 14**. The experimental data was fit with the help of software (Minitab) into a $2^{nd}$ degree regression model, and the Pareto plot, the normal effect plot and the p-value of the model terms were used to identify the significant factors affecting the response. AC for all DOE conditions were manufactured in duplicate to generate any results.

**Table 14** Limits of DOE variables for processing of zinc chloride AC from pectin

| Factor | Low | High |
|---|---|---|
| Temperature ($^{o}$C) | 400 | 600 |
| $ZnCl_2$ concentration % (w/w) | 40% | 60% |
| Mass ratio | 0.5 | 1.5 |

### 3.2.2.1 Synthesis

**Preparation of activating agent**

Aqueous solutions of zinc chloride of 40%, 50%, and 60% (w/w) concentrations were prepared by dissolving powdered zinc chloride in Milli-Q water.

**Synthesis of AC**

1 g of pectin powder was added to a beaker, depending upon the mass ratio the required volume of zinc chloride was added using a syringe and the contents were mixed together with a spatula. The mixture was then left open to atmosphere for 15 hours. Next day the mixture was transferred to a ceramic boat crucible which was then placed inside a fused quartz tube which in turn was placed inside a horizontal single zone tube furnace (Thermcraft Inc.). The furnace temperature was then ramped at 5$^{o}$C/min to the final carbonization temperature under a nitrogen atmosphere of flow rate 150 cc/min where it was maintained for another 2 hours. The furnace was then allowed to cool (<70 $^{o}$C) before the sample was taken out. Once cooled, the sample was soaked in 0.5 M HCl for 10 min to dissolve any residual zinc chloride as well as to clear out the tar blocking any pores. After that, the sample was washed with $NaHCO_3$ to remove excess HCl and washed multiple times with DI water until the pH of the washing solution was between 6 and 7. After washing the samples were dried in

an oven at 105$^{o}$C for 24 hours. The AC was then sieved following the same method as described in section 2.3.2.1.

### 3.2.2.2 Characterization

The SSA and pore size distribution of the ACs were determined using the *Quantachrome® ASiQwin* surface area analyzer using nitrogen adsorption at 77 K. The samples were degassed at 125$^{o}$ C under vacuum for 24 hours prior to measurement and the SSA was estimated using the BET method. Adsorption and desorption isotherms were generated in the relative pressure range ($P/P_0$) of 0.00025 to 1 and the linear range for the BET plot was identified using the micropore BET assistant within the Autosorb iQ software [31]. The total pore volume and pore size distribution were estimated using the QSDFT ($N_2$ equilibrium model for slit pores). Duplicate measurements were performed for each DOE sample.

Elemental analysis for the determination of carbon, hydrogen, and oxygen mass fractions was determined by combustion analysis using the *Perkin Elmer CHNS* analyzer. All samples were sent to Guelph Chemical Laboratories Limited, Canada for analysis purpose.

### 3.2.3 Scale up and additional characterization of AC made under optimized conditions

Once the optimum conditions for the maximization of SSA were identified, the process was scaled up 3 times and AC was manufactured under those conditions using the same production method as outlined in section 3.2.2.1. 17 batches of AC were manufactured and mixed together and this bulk batch of AC was then analyzed to

determine its physical and chemical properties. The different characterization techniques used are described below.

### 3.2.3.1 Specific surface area and pore size distribution

The SSA, pore volume, and pore size distribution were determined using gas sorption following the same method as outlined in section 3.2.2.2.

### 3.2.3.2 Surface morphology, Elemental analysis, Particle size, and Bulk density

SEM was employed to study the surface morphology of the AC. The AC was spread on double sided copper tape and coated with 3 nm platinum via sputter coating prior to analysis which was imaged using the FEI Magellan 400 SEM. Accelerating voltage was maintained at 1 kV and working distances used were 1-3 mm.

The carbon, hydrogen, and oxygen mass fractions were determined by combustion analysis. All samples were sent to Guelph Chemical Laboratories Limited, Canada for analysis purpose, where the analysis was done using the *Perkin Elmer CHNS* analyzer.

*Malvern Mastersizer 2000* was used to determine the particle size distribution of the AC. Water was used as the dispersion phase and the refractive and absorption indices for AC were selected as 1.6 and 0.

The bulk density of the AC sample was determined by adding the sample into a 10 ml volumetric flask, followed by measuring its mass using a laboratory balance. The bulk density measured in triplicates were calculated as:

$$\text{Bulk Density } (\text{g}/cc) = \text{Weight of the sample (g)} / \text{ Volume (cc)}$$

### 3.2.3.3 Point of zero charge

The point of zero charge of the AC was determined using the pH drift method [61]. 0.01 M stock solution of sodium chloride was prepared in Milli-Q water and 25 ml aliquots were pipetted out and transferred into 6 beakers. The pH of the solutions were adjusted in the range of 2-12 using 0.5 M and 0.1 M HCl or NaOH respectively (*pH measurements were done using instrument Hannah HI552*). 50 mg of AC was then added to each of the beakers, which were then sealed at the top with parafilm and the solutions were left for stirring for 24 hours at 200 rpm. The solutions were then filtered using 1 Whatman filter paper and the pH of the filtered solutions was measured again. A graph of final vs initial pH was plotted and the point of intersection of the curve with x = y line was used to determine the point of zero charge of the AC. Measurements were done in duplicates.

### 3.2.3.4 Adsorption of heavy metals

The adsorption of heavy metals on AC is a complex process and depends on a number of factors, namely concentration of metal ions, dosage of AC, temperature, contact time and most importantly, pH. Since the primary purpose of the present study was to investigate the manufacturing conditions for production of AC from pectin, a relatively simple procedure was employed to study the adsorption behavior of the AC without performing a detailed study. Selected values of experimental parameters (pH, dosage, contact time etc.) were chosen and an isotherm experiment was conducted to evaluate the maximum adsorption capacity of the AC under those conditions.

Lead ($Pb^{2+}$) and cadmium ($Cd^{2+}$) were chosen as the model contaminants to evaluate the adsorption capacity of the AC for removal of heavy metal ions from water in batch

mode. It is well known that most metal ions precipitate out of solution as hydroxides as pH is increased, a technique in itself for removal of metals from water [62]. As a consequence, it is important to select the initial pH value carefully and also track the final pH post adsorption. This is to ensure that no significant precipitation occurred and all removal can be attributed to solely adsorption. The extent of precipitation is unique to each metal and depends on the solubility curve. Keeping that in consideration, the initial pH values were chosen as 4 for lead and 6 for cadmium based on the solubility curve of the metal ions (**Fig. 37** and **Fig. 38**). To have a baseline reference, a control experiment run was also performed using a commercial representative AC (Norit Hydrodarco 3000) for the adsorption of lead.

Stock solutions (200 ppm) for lead or cadmium were prepared in 1000 mL volumetric flasks by dissolving $PbNO_3$ (0.32g) or $CdNO_3.4H_20$ (0.55 g) in tap water. Working solutions (10-100 ppm) were prepared by serial dilution of the respective stock solutions and 100 mL of the working solution for each concentration was pipetted out into beakers. The pH of the solutions was adjusted to 4 for experiments with lead or 6 for cadmium using 0.1 N HCl or NaOH. 100 mg of AC was added to the beakers which were then sealed at the top with Parafilm and stirred at 250 rpm for 15 hours to ensure equilibrium was obtained. 5 mL aliquots from each beaker were then filtered using a 0.45 µm syringe filter and 5 mL of 4% nitric acid was added to the aliquots for analysis purposes. Duplicate runs were done for both lead and cadmium.

ICP-OES technique was used to determine the concentration of metal ions, the instrument was set to performing triplicate analysis for each sample. Prior to analysis,

calibration curves in the concentration range (10-150 ppm) were generated using serial dilution of standard solutions for both lead and cadmium (**Fig. 35** and **Fig. 36**).

While there exist various isotherm models for the fitting of adsorption data, to keep the study simple, the classical isotherm models of Langmuir and Freundlich were used to fit the experimental data. The model equations are listed in **Table 15.**

**Table 15** Model equations for Langmuir and Freundlich isotherm models

| Model | Equation |
|---|---|
| Langmuir | $Q_e = \frac{Qmax \times b \times C_e}{1 + b \times C_e}$ |
| Freundlich | $Q_e = K_F \times C_e^{\frac{1}{n}}$ |

Where:
$Q_{max}$ is maximum equilibrium adsorption capacity (mg $g^{-1}$). It is interpreted as the mass of adsorbate (mg) that is adsorbed per unit mass of the adsorbent (g)

$Q_e$ is equilibrium adsorption capacity (mg $g^{-1}$)

$C_e$ is equilibrium concentration of adsorbate in solution (mg $L^{-1}$)

b is the Langmuir constant relating to the energy of adsorption (L $mg^{-1}$)

$K_F$ (mg $^{1-1/n}$ $g^{-1}$ $L^{1/n}$) and n are Freundlich constants relating to adsorption capacity and heterogeneity (adsorption intensity) of the adsorbent.

For Langmuir isotherm, a dimensionless constant, called the separation factor is routinely employed to predict the favourability of the adsorption process [63].

$$R_L = \frac{1}{b \times C_o}$$

The process can be unfavorable ($R_L$ >1), linear ($R_L$ =1), favorable (0<$R_L$<1) or irreversible ($R_L$=0).

The fit of experimental data into the respective models was evaluated by minimizing the residual sum of square values (RSS). For the Langmuir model, the value of $Q_{max}$ from the model was compared to the experimental $Q_{max}$ values obtained and $R_L$ values were calculated to predict favourability of the adsorption process.

## 3.3 Results and Discussions

### 3.3.1 Statistical analysis of design of experiment

The DOE was conducted to determine the optimum process conditions that would maximize the SSA. The results of the SSA along with the total pore volume and elemental composition (carbon and oxygen content) are tabulated in **Table 16**.

**Table 16** Results of gas sorption and elemental analysis for DOE maximising the SSA of zinc chloride AC from pectin

| Sl. | Temp. (° C) | $ZnCl_2$ conc. % (w/w) | $ZnCl_2$ MR | SSA ($m^2$ $g^{-1}$) | Total PV (cc $g^{-1}$) | % C | % O |
|---|---|---|---|---|---|---|---|
| 1 | 400 | 40 | 0.5 | 1419 ± 22 | 0.57 ± 0.015 | 68.9 | 26.6 |
| 2 | 600 | 40 | 0.5 | 1436 ± 153 | 0.57 ± 0.059 | 69.2 | 26.2 |
| 3 | 400 | 60 | 0.5 | 1497 ± 64 | 0.62 ± 0.023 | 70.3 | 25.2 |
| 4 | 600 | 60 | 0.5 | 1320 ± 174 | 0.51 ± 0.067 | 68.8 | 26.3 |
| 5 | 400 | 40 | 1.5 | 1928 ± 33 | 1.04 ± 0.036 | 71.1 | 23.2 |
| 6 | 600 | 40 | 1.5 | 2007 ± 217 | 1.09 ± 0.118 | 71.4 | 22.9 |
| 7 | 400 | 60 | 1.5 | 2011 ± 131 | 1.10 ± 0.057 | 69.5 | 25.3 |
| 8 | 600 | 60 | 1.5 | 1845 ± 78 | 1.09 ± 0.110 | 68.8 | 26.8 |
| 9 | 500 | 50 | 1 | 2175 ± 52 | 0.98 ± 0.010 | 71.5 | 25.1 |

At low mass ratio (0.5) all the isotherms (**Fig. 26**) obtained were of type 1, based on IUPAC classification [30]. These are for pure microporous materials with pore size 0-2 nm. This was confirmed by the results in **Table 17**, where up to 99% of the total pore volume was contributed by micropores. At high mass ratio (1.5) the isotherms resembled type 1 but have a type H4 hysteresis loop indicative of capillary condensation that occurred in the mesopores during desorption. These results are also confirmed by the volume distribution where there was a decrease in the micropore volume at high mass ratio confirming the presence of mesopores. Even so, up to 98% of the total volume was still contributed by pores in the range of 0-5 nm resulting in a predominantly microporous AC.

**Table 17** Pore volume distribution of ACs from DOE for maximization of SSA of zinc chloride AC from pectin.

| **Sl.** | **Temp. (°C)** | **$ZnCl_2$ Conc. (w/w) %** | **$ZnCl_2$ MR** | **Total PV (cc $g^{-1}$)** | **% Total PV (0-2 nm)** | **% Total PV (2-5 nm)** | **% Total PV (>5 nm)** |
|---|---|---|---|---|---|---|---|
| 1 | 400 | 40 | 0.5 | 0.57 | 97.5 | 2.4 | 0.1 |
| 2 | 600 | 40 | 0.5 | 0.56 | 98.3 | 1.5 | 0.2 |
| 3 | 400 | 60 | 0.5 | 0.62 | 94.5 | 4.5 | 1 |
| 4 | 600 | 60 | 0.5 | 0.49 | 99.7 | 0.3 | 0 |
| 5 | 400 | 40 | 1.5 | 1.08 | 72 | 24.7 | 3.3 |
| 6 | 600 | 40 | 1.5 | 1.06 | 69.2 | 30.2 | 0.6 |
| 7 | 400 | 60 | 1.5 | 1.16 | 74.2 | 23.2 | 2.5 |
| 8 | 600 | 60 | 1.5 | 1.24 | 55.3 | 40.2 | 4.4 |

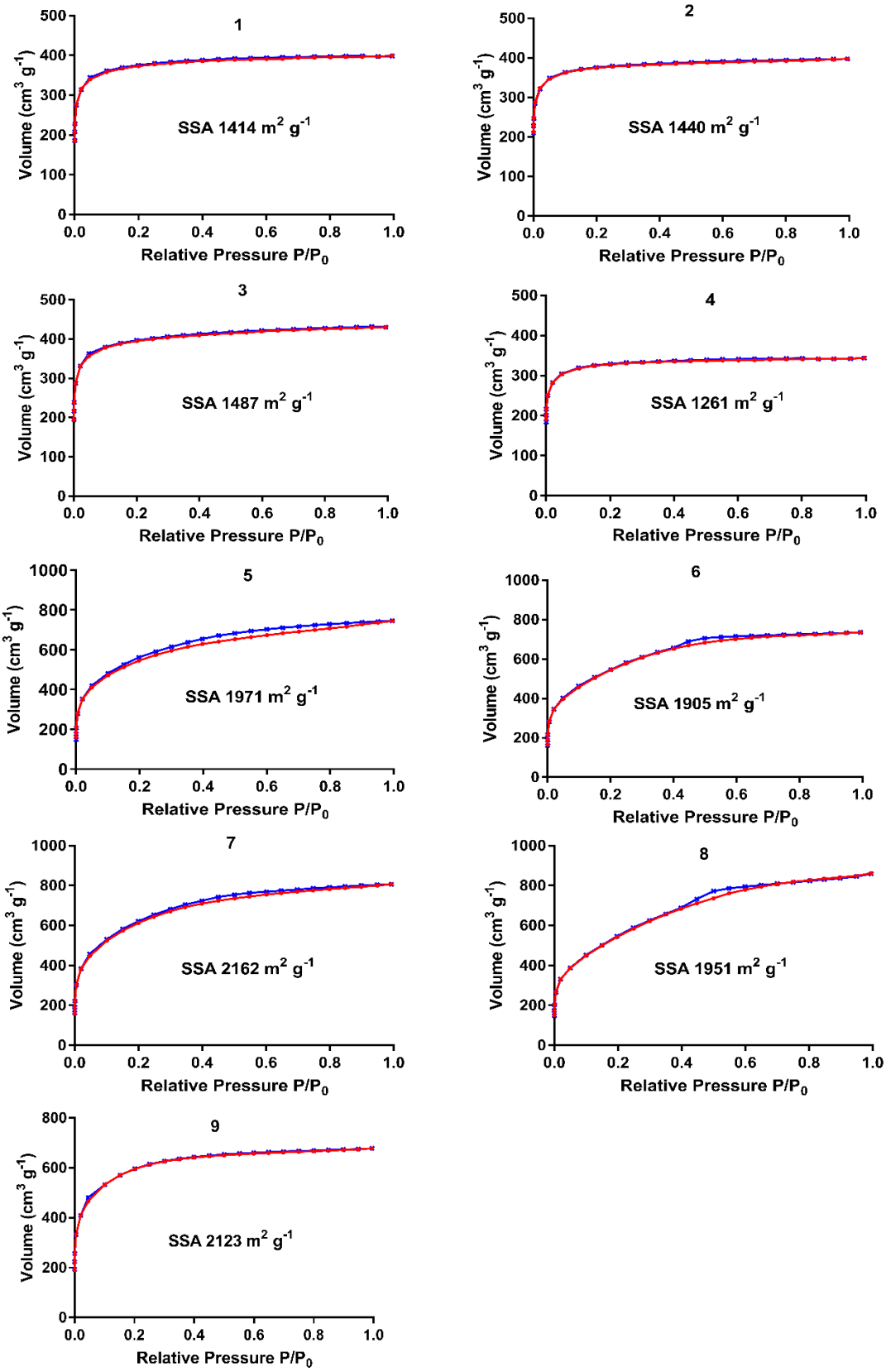


**Figure 26** Gas sorption isotherms of ACs from DOE for maximization of SSA for zinc chloride AC from pectin. Serial numbers (1-9) indicate the DOE conditions corresponding to Table 16.

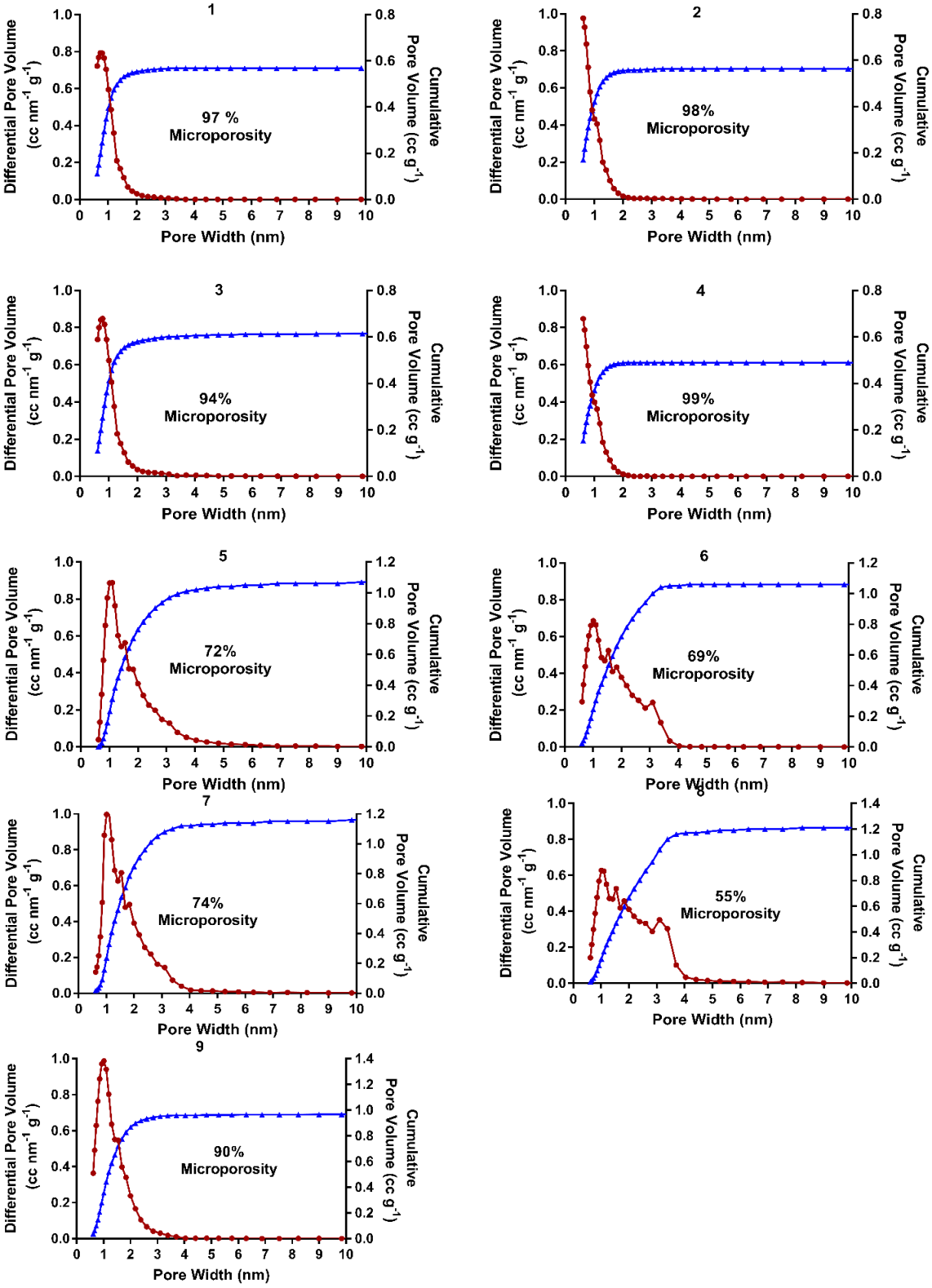


**Figure 27** Pore size distribution of ACs from DOE for maximization of SSA for zinc chloride AC from pectin. Serial numbers (1-9) indicate the DOE conditions corresponding to Table 16.

The elemental analysis data confirmed that under all conditions the chemical composition of the final AC remained relatively constant and any variations in the SSA results were purely structural. The SSAs obtained were in the range of 1400 $m^2$ $g^{-1}$ to 2200 $m^2$ $g^{-1}$. Based on the Pareto plot (**Fig. 28**), normal effect plot and the p-values of the model terms from ANOVA (**Table 18**), only the mass ratio ($p < 0.05$) had any significant effect on the SSA.

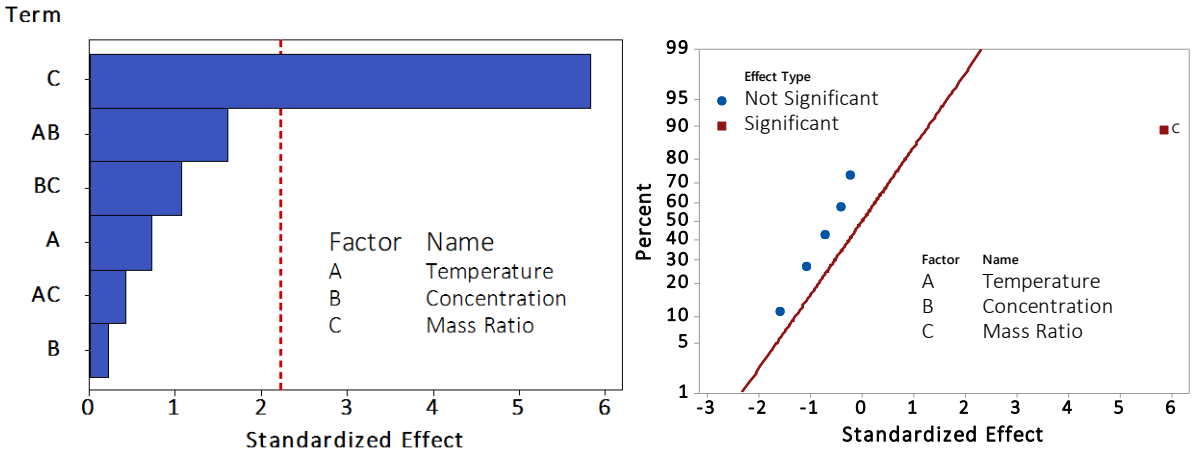


**Figure 28** The Pareto plot (left) and normal effect plot (right) revealed that the MR was the only significant factor affecting the SSA of zinc chloride AC from pectin.

**Table 18** ANOVA table for DOE maximizing the SSA of zinc chloride AC from pectin

| Source | DF | Adj SS | Adj MS | F-Value | P-Value |
|---|---|---|---|---|---|
| Model | 6 | 1268120 | 211353 | 3.23 | 0.044 |
| Linear | 3 | 1139347 | 379782 | 5.80 | 0.013 |
| Temperature | 1 | 17161 | 17161 | 0.26 | 0.619 |
| Concentration | 1 | 1764 | 1764 | 0.03 | 0.873 |
| **Mass Ratio** | **1** | **1120422** | **1120422** | **17.10** | **0.002** |
| 2-Way Interactions | 3 | 128773 | 42924 | 0.66 | 0.596 |
| Temperature*Concentration | 1 | 84972 | 84972 | 1.30 | 0.279 |
| Temperature*Mass Ratio | 1 | 5776 | 5776 | 0.09 | 0.772 |
| Concentration*Mass Ratio | 1 | 38025 | 38025 | 0.58 | 0.462 |
| Error | 11 | 720860 | 65533 | | |
| Curvature | 1 | 392502 | 392502 | 11.95 | 0.006 |
| Lack-of-Fit | 10 | 328358 | 32836 | * | * |
| Total | 17 | 1988980 | | | |

Since a major driving force for this study was to keep the process conditions less severe, the carbonization temperature and $ZnCl_2$ concentration were fixed at 400 $^oC$ and 40% respectively and the study was continued to study the effect of mass ratio on the SSA. Even at low MR (0.5) the SSAs obtained were quite high exceeding 1000 $m^2 g^{-1}$, and as the MR was increased so did the SSA, reaching a plateau then dropping a little (**Fig. 29**). The pore volume distribution obtained was similar to the DOE results, as the mass ratio was increased there was a steady drop in micropore volume and increase in mesoporosity (**Fig. 29**). The maximum SSA obtained was 2464 $m^2 g^{-1}$ at a MR of 1.25. This condition was finalized (temp. 400$^o$ C, MR 1.25, $ZnCl_2$ conc. 40%) as the optimum condition to make any future AC samples.

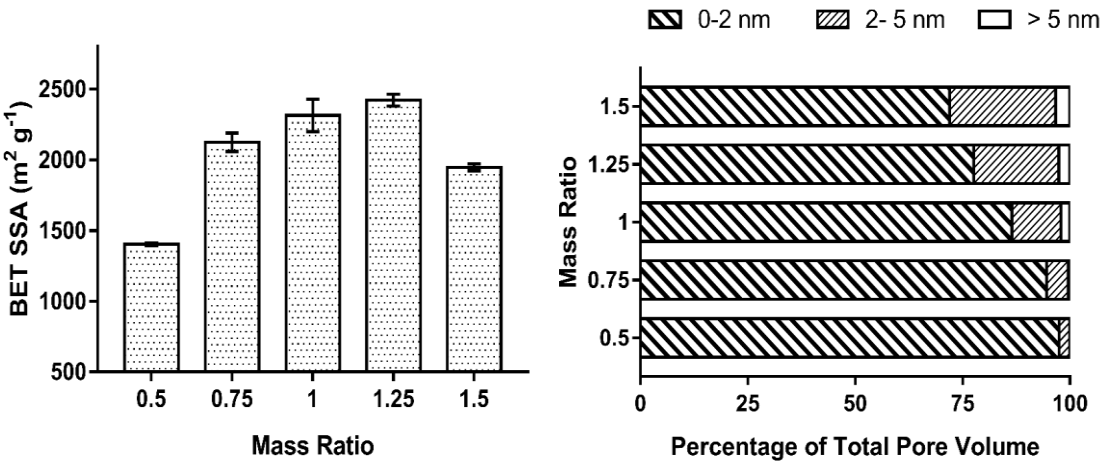


**Figure 29** The effect of MR on the SSA (left) and PV distribution (right) on zinc chloride activated carbon from pectin

Previous works have reported that during the impregnation step, $ZnCl_2$ penetrates to the interior of the particles causing hydrolysis of the parent polymer network which results in the exit of volatiles, weakening of polymer network, increase in elasticity and swelling of the particles [64]. While during the carbonization stage, $ZnCl_2$ is reported to prevent pyrolysis products such as tar and causes hydrogen and oxygen

molecules to be removed as water rather than large hydrocarbons thus leaving behind a largely untouched carbon skeleton [25]. At low mass ratios, $ZnCl_2$ can be uniformly distributed throughout the interior of the particle thus producing AC with uniform microporosity. At high mass ratios, however, even though greater swelling is observed the large quantity of $ZnCl_2$ cannot be uniformly distributed in the interior of the particles and a more heterogeneous pore distribution is observed with the development of mesopores and macropores [64]. The DOE results provide strong evidence in favor of previously reported observations.

### 3.3.2 Characterization of activated carbon made under optimum conditions

The optimum conditions identified for the manufacture of AC using zinc chloride were a $ZnCl_2$ concentration of 40%, a mass ratio of 1.25 and a carbonization temperature of 400 $^oC$. The 17 different batches of AC made under these conditions were mixed together and analyzed for physical and chemical characterization. The results from the characterization techniques are discussed below.

#### 3.3.2.1 Specific surface area and pore size distribution

The mean SSA obtained was 2049 ± 52 $m^2\ g^{-1}$ with a total pore volume of 1.09 ± 0.045 cc $g^{-1}$. Similar isotherm (resembling type 1 with an H4 hysteresis loop) and pore size distribution curves were obtained (**Fig. 30**) as during the DOE with up to 98 % of the total pore volume being contributed by pores in the size range of 1-5 nm, indicating a high degree of microporosity (78%). The observed drop in surface area can be explained due to the fact that the process had been scaled up three times and a total of 17 different batches were mixed together before performing any analysis.

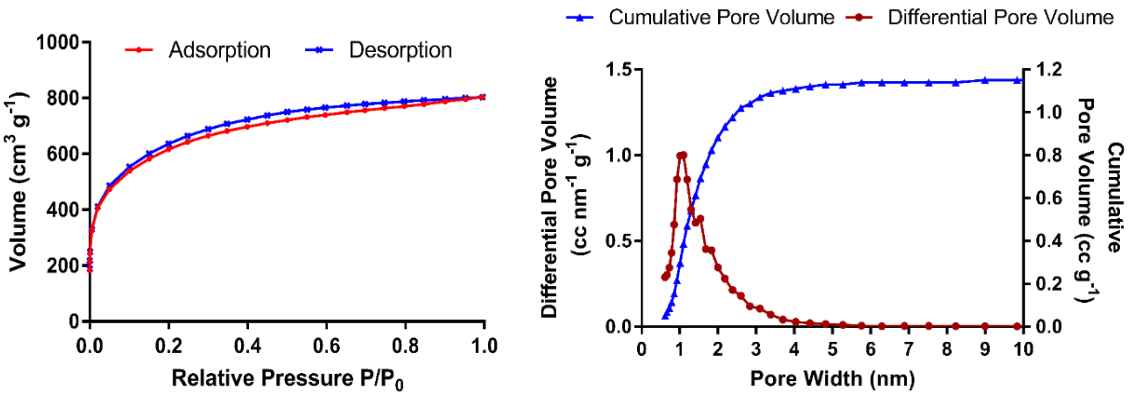


**Figure 30** Gas sorption isotherm (left) and pore size distribution (right) of AC made under optimized conditions

### 3.3.2.2 Surface morphology, Particle size, Elemental analysis, and Bulk density

The morphology of the AC was visualized through the SEM (**Fig. 31**) which was indicative of a highly porous, well-developed network of pores throughout the surface of the AC. These nano-sized pores were responsible for contributing to extensive internal surface areas as confirmed by the gas sorption results.

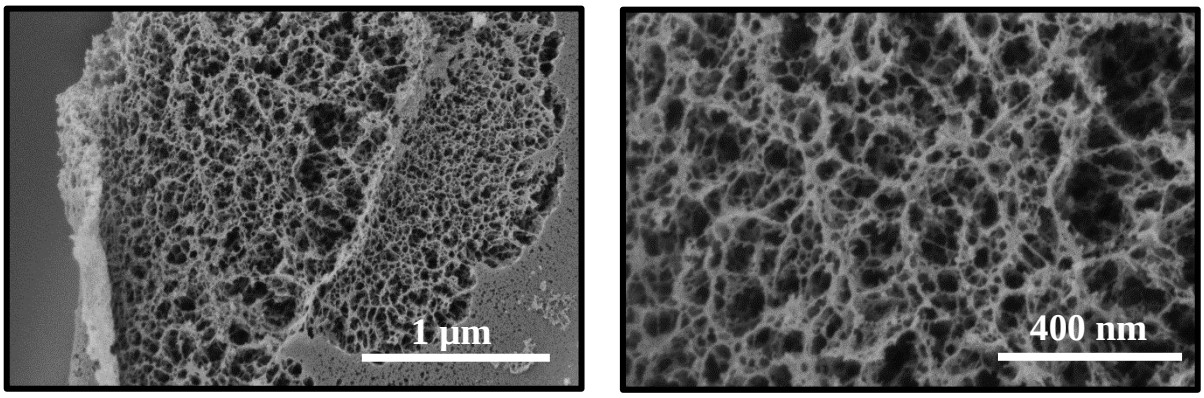


**Figure 31** SEM images of AC made under optimized conditions representing a well developed network of nano-sized pores

The particle size distribution curve is presented in **Fig. 32**. The statistics of the distribution are calculated from the results using the derived diameters based on

British standard BS2955:1993. D(0.5), D(0.1) and D(0.9) are the standard percentile readings from the analysis where D(0.5) is the size in microns at which 50% of the sample is smaller and 50% is larger. This value is also known as the mass median dameter. Similarly, D(0.1) is the size of the particle below which 10% of the sample lies and D(0.9) is the size of the particle below which 90% of the sample lies. The values obtained are presented below:

D(0.1) = 164 µm

D(0.5) = 376 µm

D(0.9) = 745 µm

It should be pointed out that since 30x80 mesh fraction was used for analysis purpose, the values of D(0.5) obtained is within the range of the individual mesh opening sizes which are 595 µm (#30) and 177 µm (#80).

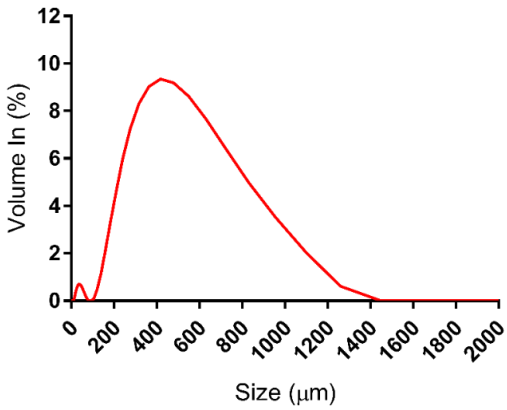


**Figure 32** Particle size distribution of AC made under optimized conditions

Due to its highly porous structure, the AC had a very low bulk density of 0.21 g $cc^{-1}$. The elemental composition of pectin before carbonization had 42% carbon, 7% hydrogen, 50% oxygen and trace quantities of nitrogen (<1%). Post carbonization the carbon content to increase to 70% and there was still 23% oxygen content in the final

form indicating that there are several oxygenated functional groups (carboxylic acids, alcohol, ester etc.) still present in the AC that will influence its adsorption behavior.

#### 3.3.2.3 Point of zero charge

The point of zero charge is a crucial characterization technique as it allows to understand the nature of charge on the AC surface under different pH conditions. A property that helps to identify the optimum conditions under which the AC will behave as a superior adsorbent. It also helps in understanding charge based attraction or repulsion that may occur between the AC surface and the target contaminant. For the AC in the study, the point of zero charge determined by pH drift method was found to be 6 (**Fig. 33**). This would mean that for pH values above 6 the surface of the adsorbent will be negatively charged and for pH below 6, it would be positively charged. The relative magnitude of positive and negative charge (surface charge density) on the surface at different pH values can be determined but was beyond the scope of this study.

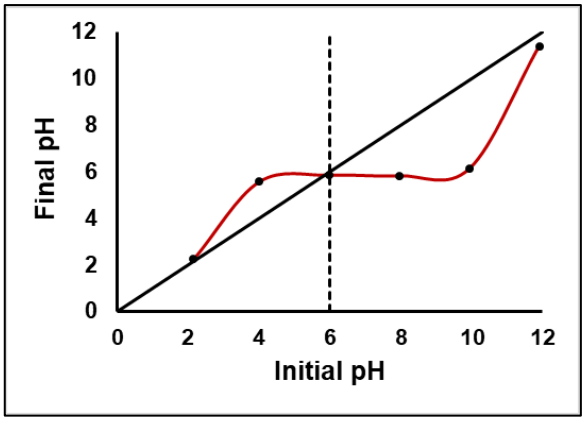


**Figure 33** Determination of point of zero charge. The dotted line (in this case ~6) represents the point of zero charge of the AC made under optimized conditions

### 3.3.2.4 Adsorption of heavy metals

Since the experimental parameters were not optimized prior to conducting the isotherm study, the values obtained do not represent the maximum possible capacities for the AC. The adsorption isotherm curves and constants are presented in **Fig. 34** and **Tables 19** and **20**.

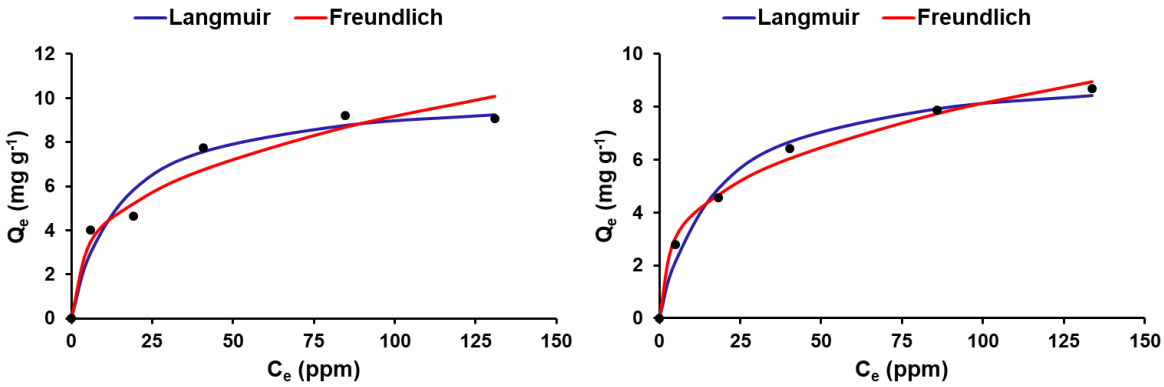


**Figure 34** Adsorption isotherms for lead (left) and cadmium (right)

**Table 19** Adsorption isotherm constants for lead ($Pb^{2+}$) removal using AC made under optimized conditions

| **Langmuir Model** | | |
|---|---|---|
| **$Q_{max}$ (mg g$^{-1}$)** | **b ( L mg$^{-1}$)** | **RSS** |
| 10.27 | 0.068 | 2.8 |
| **Freundlich Model** | | |
| **$K_F$ (mg $^{1-1/n}$ g$^{-1}$ L$^{1/n}$)** | **n** | **RSS** |
| 1.88 | 2.9 | 2.8 |

**Table 20** Adsorption isotherm constants for cadmium ($Cd^{2+}$) removal using AC made under optimum conditions

| **Langmuir Model** | | |
|---|---|---|
| **$Q_{max}$ (mg g$^{-1}$)** | **b ( L mg$^{-1}$)** | **RSS** |
| 9.49 | 0.056 | 0.72 |
| **Freundlich Model** | | |
| **$K_F$ (mg $^{1-1/n}$ g$^{-1}$ L$^{1/n}$)** | **n** | **RSS** |
| 1.8 | 3.06 | 0.29 |

The experimental values of the maximum equilibrium adsorption capacities for $Pb^{2+}$ and $Cd^{2+}$ were found as 9.2 mg $g^{-1}$ and 8.6 mg $g^{-1}$. Under the same conditions, the commercial AC gave adsorption capacity of 1.6 mg $g^{-1}$ for $Pb^{2+}$. Although it is unfair to compare ACs one to one basis on a set of results under one set of specific conditions it does give us a good foundation to design more complex studies.

The experimental data fit both the Langmuir and Freundlich isotherm models with high degree of confidence. Looking at the RSS, it was difficult to predict that the adsorption kinetics follows one of the two models. Given the relatively low concentration range, the experiments were conducted at, either of the models fit the experimental data and adsorption experiments at higher concentrations are required to find the actual kinetics.

The separation factor ($R_L$) values for Langmuir isotherm lied in the range of 0.65-0.1 for both lead and cadmium and indicating that the adsorption was favorable and the process was more favorable at lower concentrations since at higher concentrations there is saturation of the adsorbent surface leading to less number of favorable adsorption sites.

The value of Freundlich constant n is a measure of surface heterogeneity. The closer the value of 1/n to zero, the more heterogeneous the surface. A value of 1/n >1 indicates chemisorption, while <1 indicates co-operative (physical adsorption) adsorption which appeared to be the case in out results.

## 3.4. Conclusions

The present work investigated the possibility of creating high surface area AC from naturally abundant polysaccharide pectin. The study investigated the process conditions for maximizing the SSA and well as characterizing the physical and chemical properties.

It was found out that the among the process conditions, the mass ratio of the activating agent ($ZnCl_2$) was the only significant factor contributing to the surface area or the pore volume. The AC obtained was predominantly microporous although there is the possibility of tuning the pore size distribution by varying the mass ratio. On further characterizing the AC, through elemental analysis and point of zero charge measurements it was found out that the AC surface is rich in oxygenated groups. Although there is a large scope for optimization, preliminary adsorption experiments showed promising adsorption capacity for heavy metal removal from water.

# CHAPTER 4: Conclusions and Future Works

## 4.1 Conclusions

The growing demand for AC for various environmental applications has spurred a great amount of interest among researcher to find sustainable alternatives to coal for its production. This work provides an insight into the possibility of polysaccharides (starch and pectin in particular) for the manufacture of AC using conventional techniques of production. A significant amount of emphasis was given to the possibility of using PGX processed polymers for producing these carbon materials.

In chapter 2 a detailed study was conducted to compare PGX processed polymers and unprocessed polymers for AC production through two different approaches. The focus of the study was to monitor any significant variations in the SSA and pore size distributions of the AC obtained. The first approach (direct carbonization) revealed that the PGX structure was not maintained during the carbonization process and the final products from both the PGX and non PGX variants had minimal or no surface area post carbonization, essentially just producing char. The second approach (chemical activation) revealed a lot about the nature of the interaction between the starting polymer and the chemical activating agent. Starch was deemed unsuitable as a raw material using phosphoric acid as activating agent since it got completely decomposed to tar. The behavior was observed with both PGX and non PGX polymers. Pectin had a slightly better response with improved SSA values under certain conditions but it was found to be extremely difficult to reproduce any results indicating that the nature of the interaction is not homogeneous and it is possible that it is heavily dependent on the mixing stage. It might have also been possible that the

mass ratios being used were towards the higher end and at lower mass ratios it might be possible to get consistent results.

The interaction between pectin and zinc chloride as an activating agent, however, was found to be extremely favorable for the production of high surface area AC with a high degree of microporosity. SSAs exceeding 2000 $m^2$ $g^{-1}$ and microporosity up to 80% were obtained under relatively mild conditions of temperature. However, as with the earlier approach, no significant variations were noticed between PGX and non PGX processed polymers

Chapter 3 focused on further investigating the process conditions for producing AC using pectin and zinc chloride. It was revealed that the mass ratio has the biggest impact on both the surface area and the porosity. It was possible to manufacture AC with extremely high micro porosity (~100%) just by varying the mass ratio. There existed some degree of tunability in the pore size distribution although the AC was primarily microporous. Once the optimum conditions for maximising the SSA had been identified, it was followed by comprehensively characterizing the AC. Elemental analysis revealed the AC to have ~25% oxygen indicating a high degree of surface functionality. The SEM analyses showed a highly webbed network of nano sized pores. The AC was also tested for removal of heavy metal ions from water ($Pb^{2+}$, $Cd^{2+}$) and the preliminary adsorption results showed promising adsorption capacities.

## 4.2 Future works

While the present work has given us a brief insight on the use of polysaccharides (starch and pectin) for production of AC, there exists the tremendous potential for exploring both, the process parameters and the final applications in detail. Some of which are discussed below

### 4.2.1 Other polysaccharides and activating agents

The present study focused on two polysaccharides (starch and pectin) as the raw materials and two activating agents (phosphoric acid and zinc chloride). Other common polysaccharides that could be tested include chitosan, alginic acid, and cellulose while other activating agents include potassium hydroxide, boric acid, sulphuric acid, potassium chloride and, sodium hydroxide. It would be interesting to study the interaction between the many possible combinations. Similarly, the effect of different source of pectin or the different varieties of starch could be an interesting study. Physically ACs using $CO_2$ or steam are known to be mechanically stronger than chemically ACs due to the high temperature requirements, it would worth studying the variation in surface morphology and pore size distribution of these ACs compared to the chemically activated ones.

### 4.2.2 Cross-linked PGX polymers

While there did appeared to be no significant difference between the PGX and non PGX processed polymers post carbonization, primary due PGX polymers offering no additional thermal stability, it was using only the base polymers. It might to possible to crosslink the parent polymer inside or prior to entering the PGX vessel to obtain a

much more resilient and thermally stable polymer. Under these conditions, it could be possible to maintain the PGX structure during the carbonization stage, which is primarily mesoporous giving us mesoporous AC.

### 4.3.3 Additional characterization

The AC obtained through zinc chloride activation was revealed to have a high degree of surface functionality due to the presence of a significant proportion of oxygen. It would be interesting to be able to identify those functional groups, as it would allow the possibility of performing numerous post carbonization modification on the carbon for maximising its performance for an intended application. X-ray diffraction (XRD) study would be useful to identify the crystalline structure of the AC and the changes that occur with variation in temperature. Electrochemical applications typically requires a high degree of crystallinity and such a study would provide useful insight into it. Boehm titration method would be useful in quantifying the acidic and basic groups of the AC. Only a limited range of mass ratios was tested in this study and it might be possible to further optimize the process by lowering the mass ratios to a minimum value without having a significant effect on the SSA values.

### 4.3.4 Batch adsorption optimization and continuous adsorption studies

Only a preliminary adsorption study was conducted under this project. There remains to be done a vast number of optimization studies for the identification of optimum dosage, temperature, and contact time for maximizing the adsorption capacity. Additionally, kinetic and thermodynamic studies are required to understand the nature of adsorption between the AC and the adsorbate. Since AC has a higher affinity for adsorbing organic molecules, other contaminants of focus should be disinfection by

products (DBPs), like trihalomethane (THM) and haloacetic acids (HAA). Once sufficient data based on batch tests have been obtained, the AC should also be tested for use in fixed bed adsorption column for continuous operation to generate breakthrough curves and for determination of pressure drop across the column during operation. The high degree of microporosity could be useful in gas phase applications and the AC should definitely be tested for either gas storage or gas adsorption applications.

### 4.3.5 Scale up and recovery of activating agent

The scale of production in this study was limited by the size of the tube furnace. While a minor scale up was done during the production of optimized AC, it would be interesting to study how scaling up the process for example 100 times would effect the SSA and pore size distribution. Scaling up of the process will also allow the possibility of leaching out the residual zinc chloride post carbonization in sufficient quantities and reusing it.

### 4.3.6 Economic analysis

Since the ultimate aim of the project is to determine if polysaccharides can be a feasible alternative to coal as a potential replacement for the production of AC, it is extremely important to perform economic analysis for the entire process. While no process changes during the manufacturing have been proposed when using non PGX processed polymers, if PGX polymers are to be used, there will be an additional cost that will have to be considered during the analysis. The current study concluded that pectin is a suitable alternative for the manufacture of high surface area microporous AC. Pectin at this time lacks the market supply and demand compared to that of coal.

Since pectin is currently employed in the food industry the production process needs to meet good manufacturing practices and typically the final product is of high purity. This makes it unsuitable for pectin to be sold at the same low prices as that of coal. However, for the producers who do indeed manufacture pectin on a large scale for non food applications, the cost of manufacturing is reasonable low and there are currently a couple of suppliers in e-commerce website like Alibaba that are able to provide competitive prices for pectin that can match the price of coal. So it is indeed possible to make commercial grade AC from pectin while being economically competitive.

# APPENDIX

## A.1 Analysis of gas sorption data (SSA, PV and pore size distribution) of commercial ACs

Five different commercial ACs were obtained and gas sorption analysis was performed for determination of SSA, PV and pore size distribution.

**Table 21** Gas sorption analysis of commercial ACs

| Sl. | AC | SSA ($m^2 g^{-1}$) | Total PV ($cc\ g^{-1}$) | % Micropore | % Mesopore | Intended Application |
|---|---|---|---|---|---|---|
| 1 | Norit Hydrodarco 3000 | 1075 | 1.14 | 34 | 66 | Water Treatment |
| 2 | Norit Hydrodarco C | 558 | 0.61 | 29 | 71 | Water Treatment |
| 3 | Norit Vapure 410 | 1078 | 0.53 | 81 | 19 | Gas Purification |
| 4 | Norit Varpure 612 | 928 | 0.48 | 72 | 28 | Gas Purification |
| 5 | Hydrocarb | 1101 | 0.569 | 73 | 14 | Water Treatment |

## A.2 Calibration curves for ICP-OES

- Calibration curve for lead ($Pb^{2+}$)

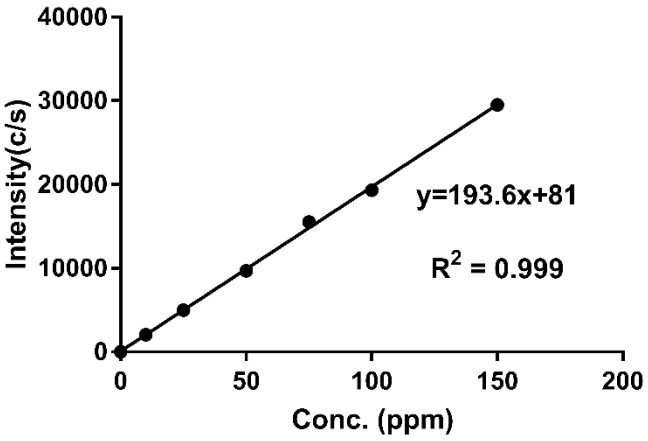


**Figure 35** ICP-OES calibration curve for lead

- Calibration curve for cadmium ($Cd^{2+}$)

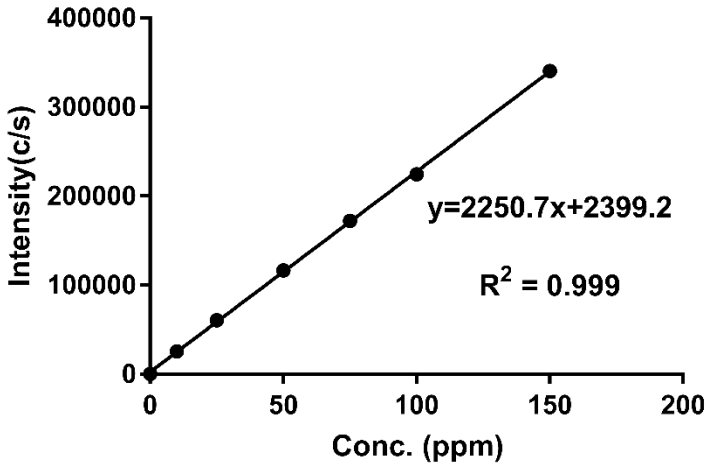


**Figure 36** ICP-OES calibration curve for cadmium

### A.3 Solubility curves for lead (II) and cadmium (II)

The solubility curves for metal ions were generated using the software Medusa, which was developed by the department of chemistry, KTH Royal Institute of Technology, Stockholm, Sweden.

- Solubility curve for lead ($Pb^{2+}$)

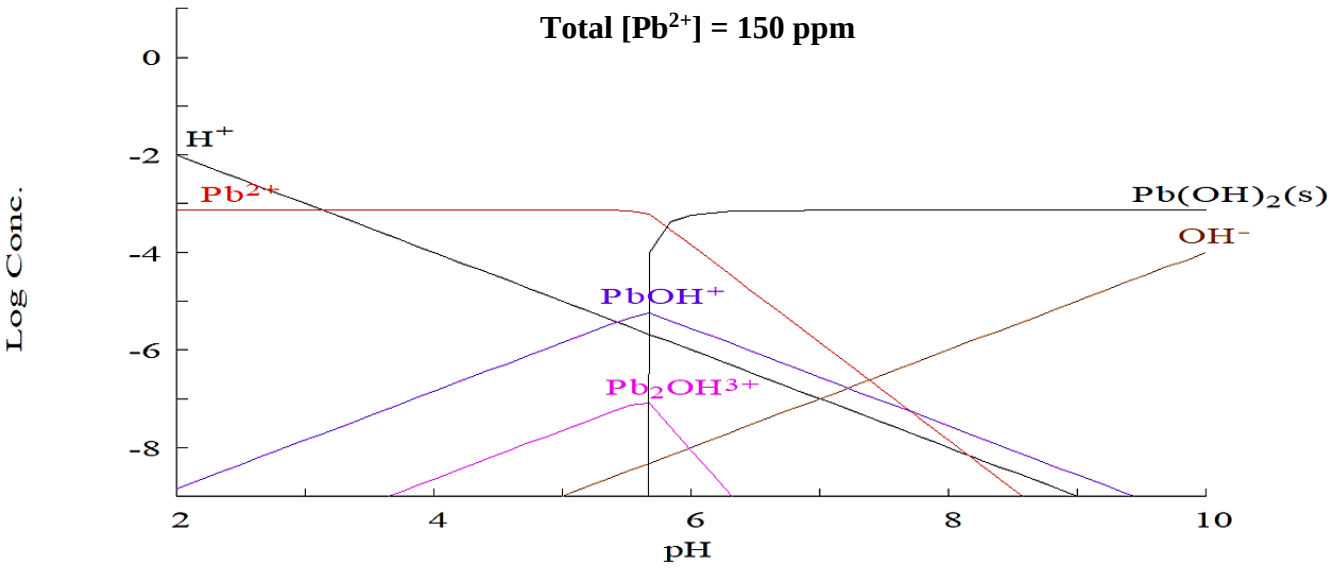


**Figure 37** Solubility curve for lead

- Solubility curve for cadmium ($Cd^{2+}$)

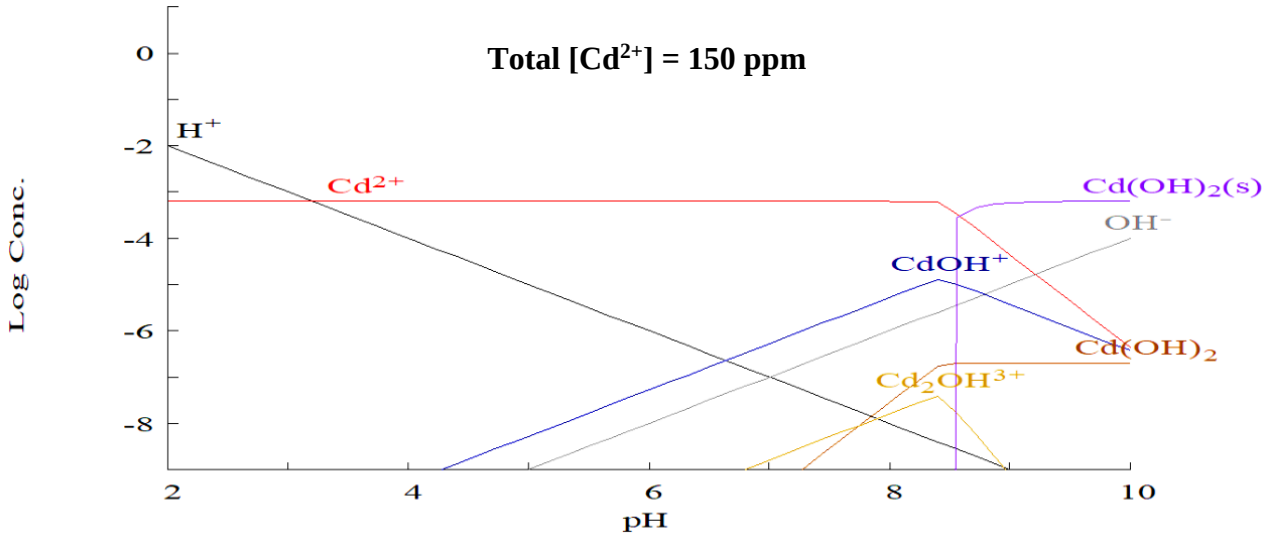


**Figure 38** Solubility curve for cadmium

### A.4 Comparative performance of commercial ACs for removal of lead from water

A batch adsorption test was conducted to compare the performance of 3 different commercial ACs for the removal of $Pb^{2+}$ from water. The experimental conditions are presented in **Table 22** and results are presented in **Fig. 39.**

**Table 22** Experimental conditions for adsorption study comparing commercial ACs

| Parameter | Value |
|---|---|
| Feed concentration (ppm) | 10 |
| AC dosage (mg) | 100 |
| Adsorption time (hrs.) | 4 |
| Stirrer speed (rpm) | 250 |
| Feed volume (ml) | 25 |
| Feed pH | 4-8 |

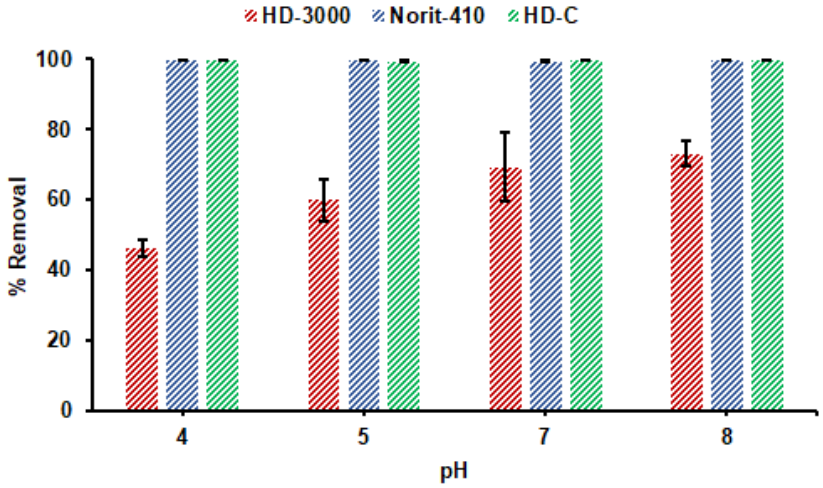


**Figure 39** Lead removal efficiencies of commercial ACs

It would appear from the results that Norit-410 and Hydrodarco-C (HD-C) have performed exceptionally well with almost 100% removal efficiency. However, it is not the case here. As previously pointed out it is extremely important to monitor the pH of the solutions during the adsorption process. The initial pH of the solutions was in the range of 4-8 and the final pH of the solutions are presented in **Fig. 40**

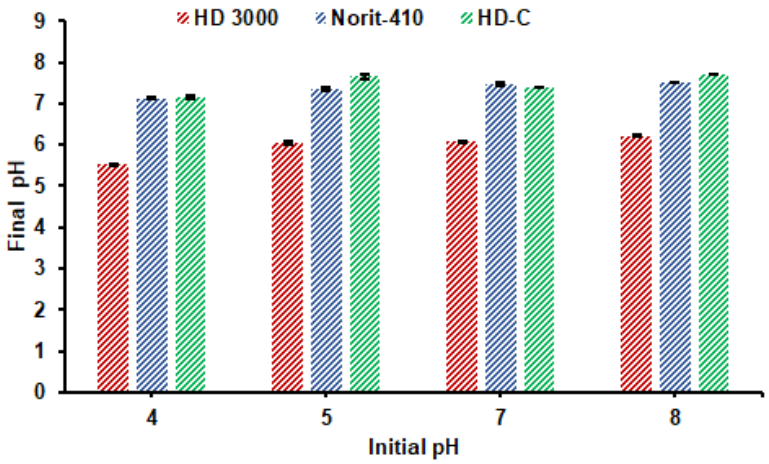


**Figure 40** Effect of different sources of AC on pH of the solution during the adsorption process

As can be seen, the final pH values for all the solutions are greater than 7 in case of Norit-410 and Hydrodarco-C even for starting pH values of 4 and 5. For a lead concentration of 10 ppm, the precipitation pH for lead is ~ 6.5. Above this pH lead has completely precipitated out of the solution in form of $Pb(OH)_2$ and the removal

efficiencies do not represent the true removal capacities of the ACs. Hence the reported values of removal efficiency where the final pH is greater than 7 do no represent the accurate adsorption capacity of the AC.

This experiment was conducted as a proof of concept that every AC is different and it is unfair to compare different ACs based on one set of conditions. The heterogeneous properties of different ACs combined with the complexity of the adsorption process, it is very important to perform a comprehensive set of experiments before establishing any conclusions. It is also important to monitor the pH values of the solutions before and after adsorption to ensure that accurate adsorption capacities are recorded and precipitation effects are taken into account. These experiments were performed prior to the adsorption experiments using in house AC so all the precautions were taken care of during those set of experiments.

# REFERENCES

[1] J. Rouquerolt, D. Avnir, C.W. Fairbridge, D.H. Everett, J.H. Haynes, N. Pernicone, J.D.F. Ramsay, K.S.W. Sing, K.K. Unger, Recommendations for the characterization of porous solids, Pure Appl. Chem. 66 (1994) 1739–1758. doi:doi:10.1351/pac199466081739.

[2] C. Moreno-Castilla, M.A. Ferro-García, J.P. Joly, F. Carrasco-Marín, J. Rivera-Utrilla, Activated Carbon Surface Modifications by Nitric Acid, Hydrogen Peroxide, and Ammonium Peroxydisulfate Treatments, 1995. https://pubs.acs.org/sharingguidelines (accessed November 9, 2018).

[3] V. Gomez-Serrano, A. MacIas-Garcia, A. Espinosa-Mansilla, C. Valenzuela-Calahorro, Adsorption of mercury, cadmium and lead from aqueous solution on heat-treated and sulphurized activated carbon, Water Res. 32 (1998) 1–4. doi:10.1016/S0043-1354(97)00203-0.

[4] L. Zhao, L.Z. Fan, M.Q. Zhou, H. Guan, S. Qiao, M. Antonietti, M.M. Titirici, Nitrogen-containing hydrothermal carbons with superior performance in supercapacitors, Adv. Mater. 22 (2010) 5202–5206. doi:10.1002/adma.201002647.

[5] S. Wang, G.Q. (Max)Lu, Effects of acidic treatments on the pore and surface properties of Ni catalyst supported on activated carbon, Carbon N. Y. 36 (1998) 283–292. doi:10.1016/S0008-6223(97)00187-5.

[6] S.. de Miguel, J.. Vilella, E.. Jablonski, O.. Scelza, C. Salinas-Martinez de Lecea, A. Linares-Solano, Preparation of Pt catalysts supported on activated carbon felts (ACF), Appl. Catal. A Gen. 232 (2002) 237–246. doi:10.1016/S0926-860X(02)00112-6.

[7] Y.S. Al-Degs, M.I. El-Barghouthi, A.H. El-Sheikh, G.M. Walker, Effect of solution pH, ionic strength, and temperature on adsorption behavior of reactive dyes on activated carbon, Dye. Pigment. 77 (2008) 16–23. doi:10.1016/j.dyepig.2007.03.001.

[8] S. Venkata Mohan, N. Chandrasekhar Rao, J. Karthikeyan, Adsorptive removal of direct azo dye from aqueous phase onto coal based sorbents: A kinetic and mechanistic study, J. Hazard. Mater. 90 (2002) 189–204. doi:10.1016/S0304-3894(01)00348-X.

[9] D. Das, V. Gaur, N. Verma, Removal of volatile organic compound by activated carbon fiber, Carbon N. Y. 42 (2004) 2949–2962. doi:10.1016/j.carbon.2004.07.008.

[10] D.M. Ayeres, A.P. Davis, P.M. Gietka, Removing Heavy Metals from Wastewater, (1994) 1–21.

[11] M.M. Rahman, M. Adil, A.M. Yusof, Y.B. Kamaruzzaman, R.H. Ansary, Removal of heavy metal ions with acid activated carbons derived from oil palm and coconut shells, Materials (Basel). 7 (2014) 3634–3650. doi:10.3390/ma7053634.

[12] M. Yates, J. Blanco, P. Avila, M.P. Martin, Honeycomb monoliths of activated carbons for effluent gas purification, Microporous Mesoporous Mater. 37 (2000) 201–208. doi:10.1016/S1387-1811(99)00266-8.

[13] H. Zeng, F. Jin, J. Guo, Removal of elemental mercury from coal combustion flue gas by chloride-impregnated activated carbon, Fuel. 83 (2004) 143–146. doi:10.1016/S0016-2361(03)00235-7.

[14] M.S. Khayoon, B.H. Hameed, Acetylation of glycerol to biofuel additives over sulfated activated carbon catalyst, Bioresour. Technol. 102 (2011) 9229–9235. doi:10.1016/j.biortech.2011.07.035.

[15] H. Shimada, T. Akazawa, N.O. Ikenaga, T. Suzuki, Dehydrogenation of isobutane to isobutene with iron-loaded activated carbon catalyst, Appl. Catal. A Gen. 168 (1998) 243–250. doi:10.1016/S0926-860X(97)00350-5.

[16] S. Biloé, V. Goetz, A. Guillot, Optimal design of an activated carbon for an adsorbed natural gas storage system, Carbon N. Y. 40 (2002) 1295–1308. doi:10.1016/S0008-6223(01)00287-1.

[17] I.I. El-Sharkawy, M.H. Mansour, M.M. Awad, R. El-Ashry, Investigation of Natural Gas Storage through Activated Carbon, J. Chem. Eng. Data. 60 (2015) 3215–3223. doi:10.1021/acs.jced.5b00430.

[18] Global and China Activated Carbon Industry Report, 2018-2023, (n.d.). https://www.researchandmarkets.com/reports/4605170/global-and-china-activated-carbon-industry (accessed November 9, 2018).

[19] Raw materials of activated carbon | Desotec, (n.d.). https://www.desotec.com/en/carbonology/carbonology-academy/raw-materials-activated-carbon (accessed December 16, 2018).

[20] R.J. White, V. Budarin, R. Luque, J.H. Clark, D.J. MacQuarrie, Tuneable porous carbonaceous materials from renewable resources, Chem. Soc. Rev. 38 (2009) 3401–3418. doi:10.1039/b822668g.

[21] F. Temelli, B. Seifried, Supercritical Fluid Treatment of High Molecular Weight Biopolymers, 2013. doi:US 2010/0311130 Al.

[22] The History of Activated Carbon - Jurassic Carbon, (n.d.). https://www.jurassiccarbon.com/blogs/news/12186281-the-history-of-activated-carbon (accessed November 22, 2018).

[23] J.A. Menéndez-Díaz, I. Martín-Gullón, Published in Activated carbon surfaces in environmental remediation (Interface science and technology series Types of carbon adsorbents and their production, 2006. http://digital.csic.es/bitstream/10261/95477/1/Types of carbon adsorbents and their producton.pdf.

[24] G.J. McDougall, Physical nature and manufacture of activated carbon, J. South African Inst. Min. Metall. 91 (1991) 109–120. http://www.scopus.com/inward/record.url?eid=2-s2.0-0026139382&partnerID=tZOtx3y1.

[25] S.J. Allen, L. Whitten, G. Mckay, The Production and Characterisation of Activated Carbons: A Review, Dev. Chem. Eng. Miner. Process. 6 (1998) 231–261. doi:10.1002/apj.5500060501.

[26] V. Chauhan, Preparation and characterization of activated carbon from biomass, Sardar Patel University, 2002. http://shodhganga.inflibnet.ac.in/handle/10603/76043.

[27] H. Giesche, Mercury porosimetry: A general (practical) overview, Part. Part. Syst. Charact. 23 (2006) 9–19. doi:10.1002/ppsc.200601009.

[28] Quantachrome Instruments, auto sorb iQ and ASiQwin GAS SORPTION SYSTEM, (2013) 365–366.

[29] Surface Area Measurement Services | Particle Testing Authority, (n.d.). http://particletesting.com/surface-area/ (accessed November 9, 2018).

[30] M. Thommes, K. Kaneko, A. V. Neimark, J.P. Olivier, F. Rodriguez-Reinoso, J. Rouquerol, K.S.W. Sing, Physisorption of gases, with special reference to the evaluation of surface area and pore size distribution (IUPAC Technical Report), Pure Appl. Chem. 87 (2015) 1051–1069. doi:10.1515/pac-2014-1117.

[31] Calculation of BET Area of Microporous Materials with Automated Software, (n.d.). https://www.azom.com/article.aspx?ArticleID=9434 (accessed December 17, 2018).

[32] E.P. Barrett, L.G. Joyner, P.P. Halenda, The Determination of Pore Volume and Area Distributions in Porous Substances. I. Computations from Nitrogen Isotherms, J. Am. Chem. Soc. 73 (1951) 373–380. doi:10.1021/ja01145a126.

[33] J. Landers, G.Y. Gor, A. V. Neimark, Density functional theory methods for characterization of porous materials, Colloids Surfaces A Physicochem. Eng. Asp. 437 (2013) 3–32. doi:10.1016/j.colsurfa.2013.01.007.

[34] Quenched Solid State Functional Theory (QSDFT) for Pore Size Analysis of Disordered Carbon, (n.d.). https://www.azom.com/article.aspx?ArticleID=5191 (accessed December 18, 2018).

[35] Chemviron, Applications - Chemviron, (n.d.). http://www.chemviron.eu/applications/ (accessed November 9, 2018).

[36] Global and China Activated Carbon Market 2017-2021 - 6 Foreign and 19 Chinese Activated Carbon Enterprises, (n.d.). https://www.prnewswire.com/news-releases/global-and-china-activated-carbon-market-2017-2021---6-foreign-and-19-chinese-activated-carbon-enterprises-300502107.html (accessed November 9, 2018).

[37] Where is coal found? | World Coal Association, (n.d.). https://www.worldcoal.org/coal/where-coal-found (accessed November 7, 2018).

[38] Y.E. Yudovich, M.P. Ketris, Mercury in coal: A review. Part 1. Geochemistry, Int. J. Coal Geol. 62 (2005) 107–134. doi:10.1016/j.coal.2004.11.002.

[39] A. Kumar, H.M. Jena, Preparation and characterization of high surface area activated carbon from Fox nut (Euryale ferox) shell by chemical activation with H3PO4, Results Phys. 6 (2016) 651–658. doi:10.1016/j.rinp.2016.09.012.

[40] A.C. Lua, T. Yang, J. Guo, Effects of pyrolysis conditions on the properties of activated carbons prepared from pistachio-nut shells, J. Anal. Appl. Pyrolysis. 72 (2004) 279–287. doi:10.1016/j.jaap.2004.08.001.

[41] A. Marcilla, S. García-García, M. Asensio, J.A. Conesa, Influence of thermal treatment regime on the density and reactivity of activated carbons from almond shells, Carbon N. Y. 38 (2000) 429–440. doi:10.1016/S0008-6223(99)00123-2.

[42] T. Zhang, W.P. Walawender, L.T. Fan, M. Fan, D. Daugaard, R.C. Brown, Preparation of activated carbon from forest and agricultural residues through CO2 activation, Chem. Eng. J. 105 (2004) 53–59. doi:10.1016/j.cej.2004.06.011.

[43] M. Fan, W. Marshall, D. Daugaard, R.C. Brown, Steam activation of chars produced from oat hulls and corn stover, Bioresour. Technol. 93 (2004) 103–107. doi:10.1016/j.biortech.2003.08.016.

[44] G.H. Oh, C.R. Park, Preparation and characteristics of rice-straw-based porous carbons with high adsorption capacity, Fuel. 81 (2002) 327–336. doi:10.1016/S0016-2361(01)00171-5.

[45] Y. Sudaryanto, S.B. Hartono, W. Irawaty, H. Hindarso, S. Ismadji, High surface area activated carbon prepared from cassava peel by chemical activation, Bioresour. Technol. 97 (2006) 734–739. doi:10.1016/j.biortech.2005.04.029.

[46] S.M. Yakout, G. Sharaf El-Deen, Characterization of activated carbon prepared by phosphoric acid activation of olive stones, Arab. J. Chem. 9 (2016) S1155–S1162. doi:10.1016/j.arabjc.2011.12.002.

[47] A. Ahmadpour, D.D. Do, The preparation of activated carbon from macadamia nutshell by chemical activation, Carbon N. Y. 35 (1997) 1723–1732. doi:10.1016/S0008-6223(97)00127-9.

[48] L.S. L., Preparation and characterization of activated carbons from corn cob, Carbon N. Y. 35 (1997) 1198.

[49] D. Savova, E. Apak, E. Ekinci, F. Yardim, N. Petrov, T. Budinova, M. Razvigorova, V. Minkova, Biomass conversion to carbon adsorbents and gas, Biomass and Bioenergy. 21 (2001) 133–142. doi:10.1016/S0961-9534(01)00027-7.

[50] V.S. Nevin, Studies of the surface area and porosity of activated carbons prepared from rice husks, Carbon N. Y. 38 (2000) 1943–1945. doi:10.1016/S0022-3476(48)80245-3.

[51] Y. Weirong, Y. Huiyuan, Adsorbent characteristics of porous starch, Starch/Staerke. 54 (2002) 260–263. doi:10.1002/1521-379X(200206)54:6<260::AID-STAR260>3.0.CO;2-Z.

[52] H. Yokoi, T. Obita, J. Hirose, S. Hayashi, Y. Takasaki, Flocculation properties of pectin in various suspensions, Bioresour. Technol. 84 (2002) 287–290. doi:10.1016/S0960-8524(02)00023-8.

[53] P. Lu, Y. Lo Hsieh, Cellulose nanocrystal-filled poly(acrylic acid) nanocomposite fibrous membranes, Nanotechnology. 20 (2009). doi:10.1088/0957-4484/20/41/415604.

[54] N. Mahfoudhi, S. Boufi, Nanocellulose as a novel nanostructured adsorbent for environmental remediation: a review, Cellulose. 24 (2017) 1171–1197.

doi:10.1007/s10570-017-1194-0.

[55] B. Seifried, B. Seifried, Physicochemical Properties and Microencapsulation Process Development for Fish Oil using Supercritical Carbon Dioxide by Examining Committee Dr . Feral Temelli , Department of Agricultural , Food and Nutritional Science, (2010).

[56] Pressurized Gas Expanded (PGX) Technology :: Ceapro Inc., (n.d.). https://www.ceapro.com/technologies/pgx (accessed November 10, 2018).

[57] V.L. Budarin, J.H. Clark, R. Luque, D.J. MacQuarrie, A. Koutinas, C. Webb, Tunable mesoporous materials optimised for aqueous phase esterifications, Green Chem. 9 (2007) 992–995. doi:10.1039/b704055e.

[58] O. Ioannidou, A. Zabaniotou, Agricultural residues as precursors for activated carbon production-A review, Renew. Sustain. Energy Rev. 11 (2007) 1966–2005. doi:10.1016/j.rser.2006.03.013.

[59] P.S. Shuttleworth, V. Budarin, J.H. Clark, Green power - “molten” starch adhesives, J. Mater. Chem. 19 (2009) 8589–8593. doi:10.1039/b911342h.

[60] C.M. Lakshmanan, H.E. Hoelscher, Production of Levoglucosan by Pyrolysis of Carbohydrates. Pyrolysis in Hot Inert Gas Stream, Ind. Eng. Chem. Prod. Res. Dev. 9 (1970) 57–59. doi:10.1021/i360033a011.

[61] P.C.C. Faria, J.J.M. Órfão, M.F.R. Pereira, Adsorption of anionic and cationic dyes on activated carbons with different surface chemistries, Water Res. 38 (2004) 2043–2052. doi:10.1016/j.watres.2004.01.034.

[62] F. Fu, Q. Wang, Removal of heavy metal ions from wastewaters: A review, J. Environ. Manage. 92 (2011) 407–418. doi:10.1016/j.jenvman.2010.11.011.

[63] N. Ayawei, A.N. Ebelegi, D. Wankasi, Modelling and Interpretation of Adsorption Isotherms, J. Chem. 2017 (2017). doi:10.1155/2017/3039817.

[64] F. Rodríguez-Reinoso, M. Molina-Sabio, Activated carbons from lignocellulosic materials by chemical and/or physical activation: an overview, Carbon N. Y. 30 (1992) 1111–1118. doi:10.1016/0008-6223(92)90143-K.